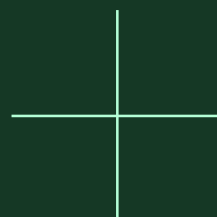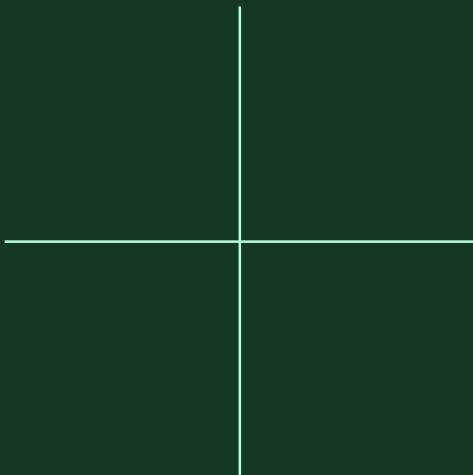# ARV
CLIMATE POSITIVE CIRCULAR COMMUNITIES

D7.6 GUIDELINES ON DESCRIPTIONS OF SMARTNESS AND FLEXIBILITY

WP7 EFFICIENT OPERATION AND FLEXIBILITY

Ge Song, NTNU
Natasa Nord, NTNU
Henrik Madsen, DTU
Jan Eric Thorsen, Danfoss
Seyed Shahabaldin Tohidi, DTU
Reza Mokhtari, DTU
Khadija Barhmi, Utrecht University
Sofiane Kichou, CVUT
Tomas Baumelt, CVUT

PROJECT INFORMATION

Project acronym	**ARV[1]**
Project title	Climate Positive Circular Communities
Project number	101036723
Coordinator	Norwegian University of Science and Technology / Inger Andresen
Website	www.GreenDeal-ARV.eu

DOCUMENT INFORMATION

Deliverable Number and Title	**D.7.6 Guidelines on description of smartness and flexibility**			
Due Month	M24			
Work Package Number and Title	WP 7. Efficient Operation and Flexibility			
Task number and Title	Task 7.6 Describe energy flexibility functions and measures			
Dissemination Level	PU = Public, fully open			
Date of Delivery	31.12.2023			
Lead Author	Ge Song, Norwegian University of Science and Technology (NTNU)			
Contributors	Natasa Nord (NTNU), Henrik Madsen (DTU), Jan Eric Thorsen (DANFOSS), Seyed Shahabaldin Tohidi (DTU), Reza Mokhtari (DTU), Khadija Barhmi (UU) , Sofiane Kichou (CVUT), Tomas Baumelt (CVUT)			
Reviewers	Sergio Romero Salas, ENFOR			
Status	Final version V.02			
Revision Log	**Version**	**Authors**	**Main changes**	**Date**
	V.01	Ge Song (NTNU), Natasa Nord (NTNU), Henrik Madsen (DTU), Jan Eric Thorsen (DANFOSS), Seyed Shahabaldin Tohidi (DTU), Reza Mokhtari (DTU), Khadija Barhmi (UU), Sofiane Kichou (CVUT), Tomas Baumelt (CVUT)	First Draft Second Draft	13.12.2023 21.12.2023
	V.02	Sergio Romero Salas (ENFOR) and Razgar Ebrahimy (DTU)	Review	22.12.2023

---

[1] *ARV is a Norwegian word meaning "heritage" or "legacy". It reflects the emphasis on circularity, a key aspect in reaching the project's main goal of boosting the building renovation rate in Europe.*
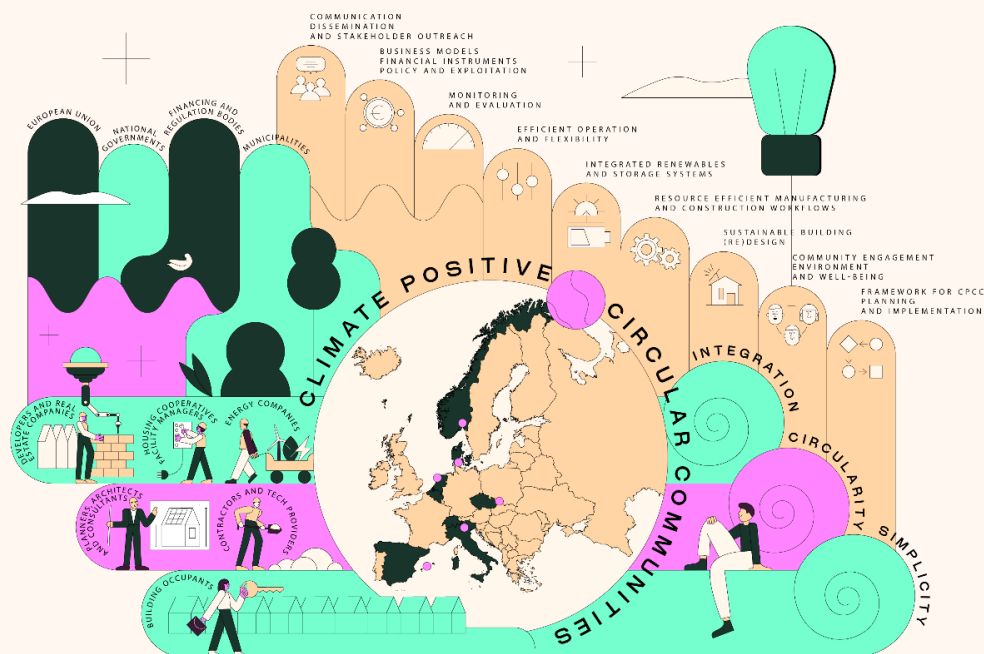
ABOUT THE ARV PROJECT

The vision of the ARV project is to contribute to speedy and wide scale implementation of Climate Positive Circular Communities (CPCC) where people can thrive and prosper for generations to come. The overall aim is to demonstrate and validate attractive, resilient, and affordable solutions for CPCC that will significantly speed up the deep energy renovations and the deployment of energy and climate measures in the construction and energy industries. To achieve this, the ARV project will employ a novel concept relying on a combination of 3 conceptual pillars, 6 demonstration projects, and 9 thematic focus areas.

The 3 conceptual pillars are integration, circularity, and simplicity. **Integration** in ARV means the coupling of people, buildings, and energy systems, through multi-stakeholder co-creation and use of innovative digital tools. **Circularity** in ARV means a systematic way of addressing circular economy through integrated use of Life Cycle Assessment, digital logbooks, and material banks. **Simplicity** in ARV means to make the solutions easy to understand and use for all stakeholders, from manufacturers to end-users.

The 6 demonstration projects are urban regeneration projects in 6 locations around Europe. They have been carefully selected to represent the different European climates and contexts, and due to their high ambitions in environmental, social, and economic sustainability. Renovation of social housing and public buildings are specifically focused. Together, they will demonstrate more than 50 innovations in more than 150,000 m^2 of buildings.

The 9 thematic focus areas are 1) Effective planning and implementation of CPCCs, 2) Enhancing citizen engagement, environment, and well-being, 3) Sustainable building re(design) 4) Resource efficient manufacturing and construction workflows, 5) Smart integration of renewables and storage systems, 6) Effective management of energy and flexibility, 7) Continuous monitoring and evaluation, 8) New business models and financial mechanisms, policy instruments and exploitation, and 9) Effective communication, dissemination, and stakeholder outreach.

The ARV project is an Innovation Action that has received funding under the Green Deal Call LC-GD-4-1-2020 - Building and renovating in an energy and resource efficient way. The project started in January 2022 and has a project period of 4 years, until December 2025. The project is coordinated by the Norwegian University of Science and Technology and involves 35 partners from 8 different European Countries.

EXECUTIVE SUMMARY

The aim of the report is to describe and identify energy flexibility based on the inputs from WP6 and WP5. Further the aim was to formulate the Flexibility Functions (FFs) and Flexibility Index (FI) and their relation to Smart Readiness Indicator (SRI). The report is tailored based on local flexibility for demo projects and other case studies.

The report consists of two main parts, mathematical definition of flexibility and examples how to achieve energy flexibility. These examples are given for eight different case studies. The cases given in the report are showing in excellent way how heating and electricity load may be shifted for the purpose of energy efficiency, peak load reduction, self-consumption, and link between the energy market and physical systems.

To explain flexibility concept related to energy, the deliverable starts with differing the SRI and FF. The most important difference between these two can be explained as SRI evaluates a building's holistic readiness for smart technologies, while flexibility explores the dynamic response mechanisms within energy systems, emphasizing adaptability to external factors and efficient energy use. Definition of flexibility and the FF are given in the first part of the report. The FF are important in achieving ambitious sustainability targets due to its enabling possibility within energy efficiency, peak load reduction, self-consumption, and link between the energy market and physical systems.

Examples of rule-based, model predicative control, and AI-based implementation for increase of flexibility are presented. Some of the examples are test of the real cases in simulation environment, while some of the examples are real achieved results.

Use of Leanheat Building AI-based heating control for peak shaving to increase usage of CO_2 neutral base-load heat production is given for one of the examples. Leanheat's AI learns how the building thermal mass reacts to the ambient conditions and evaluates the flexibility potential based on the forecasted weather and defined comfort requirements. Further, an example how load shifting for domestic tap water may help to even the total heat demand is given. This shows how the load shift potential appears very relevant as an additional flexibility on top of the load shift potential originating from the heating system.

By studying flexibility in buildings equipped with PV and batteries and utilizing PV forecasting, the Dutch demo case maximizes self-consumption, peak shaving, and overall energy efficiency, paving the way for effective urban energy transformation. Flexibility in PV systems means adjusting solar power generation to match dynamic grid demands, requiring advanced control strategies, predictive algorithms, and real-time monitoring. Similarly, flexibility in energy storage (batteries) involves efficient storage, discharge, and energy management.

The novel shallow energy wall system is installed in the example case in Turin, Italy, for experimental purposes to provide insight into the system energy performance and into the thermal impact that is exerted on the surrounding ground. This kind of energy system may indeed play a role in the optimisation of the geothermal resources use, allowing to efficiently mine the heat at very shallow depths even in densely inhabited areas. This system may strongly contribute to the system energy flexibility due to its possibility to store heat from renewable sources.

The Czech demo case illustrates the pivotal role of flexibility in propelling building performance beyond benchmarks. The Smart Energy Management Strategy (SEMS) was developed to further underscore the importance of flexibility, meticulously crafted to enhance sustainability and reduce operational costs. SEMS leverages flexibility in response to real-time conditions, mitigating the impact of forecasting inaccuracies and actively contributing to grid congestion alleviation through ancillary services. Simulation outcomes demonstrate the effectiveness of SEMS in significantly reducing electricity bills and enhancing flexibility, thus reinforcing the critical role that flexibility plays in the overall energy management strategy.

TABLE OF CONTENTS

1. INTRODUCTION

The aim of the ARV project in the context of energy flexibility and flexibility measures is to develop methods and tools for describing and identifying energy flexibility of building heat and electricity use. The project focuses on creating Flexibility Functions (FFs) that can provide local grid support or other power system services. These FFs are formulated with input from Work Packages 6 (WP6) and 5 (WP5), which contribute with specific expertise or data to the task.

Work package WP7 focuses on the deployment of solutions for optimizing the performance during the operation of the six demo sites in ARV. The performance will be measured by a user-oriented preference metrics related to energy efficiency, flexibility, and cost efficiency, while serious considerations are taken in the direction of energy positive districts and buildings. In the future weather-driven energy system, end-user flexibility will play an important role. The focus is on unlocking the available flexibility in demo sites for optimizing the self-consumption and minimizing the carbon footprint by data-driven and intelligent operations. Therefore, within WP7, Task 7.6 deals with the description and identification of energy flexibility based on the inputs from WP6 and WP5. Further this deliverable aims to formulate the FFs and Flexibility Index (FI) and their relation to Smart Readiness Indicator (SRI). The report is tailored based on local flexibility for demo projects and other case studies.

The objectives of the deliverable D7.6. are to introduce the FF and give examples of flexibility potentials in ARV demo cases or other cases by giving description how to evaluate energy flexibility for different systems. The FF is firstly defined as a mean for flexibility exploration of the dynamic response mechanisms within energy systems, emphasizing adaptability to external factors, improved energy efficiency, cost savings, and sustainability.

The report consists of two main parts, mathematical definition of flexibility and examples how to achieve energy flexibility. The most important for this deliverable is to present methodologies for flexibility evaluation and implementation. The examples in the deliverable D7.6 are given for eight different case studies. Three examples are covering two demo cases, Sønderborg in Denmark, Utrecht in Netherlands, Karvina in Czechia. Results on energy flexibility are not given for the demo case Oslo in Norway, because the building is since recently in operation and no operation data are available. For the case in Trento, Italy, only example that the system may provide heat flexibility is explained through a laboratory test in Turino, Italy. However, the eight cases given in the report are showing in excellent way how to unlock the available flexibility in all the ARV demo sites for optimizing the self-consumption and minimizing the carbon footprint by data-driven and intelligent operations. The given eight examples in the deliverable are covering the same climatic are as the demo cases in the ARV project. Since the deliverable D7.6 has deadline M24, which is mid of the ARV project, and is dependent on the demo case operation data, it has been difficult and, in some cases, impossible to obtain real data for the flexibility evaluation. Finally, the methods, findings, and examples from the deliverable D7.6 will be used for the flexibility evaluation and documentation in other parts of the project, such as WP6 to document demo cases and WP7 for further operation optimization.

The deliverable D7.6 should be used as an instruction document for flexibility evaluation and implementation for the other demos in the ARV project.

2. SMART READINESS INDICATORS DEFINITION

The Smart Readiness Indicator (SRI) serves as a pivotal tool, meticulously designed to gauge a building's capacity in effective way by utilizing information and communication technologies (ICT) and electronic systems. At its core, the SRI aims to adapt building operations dynamically, catering to the ever-changing needs of occupants and grid demands, all while enhancing energy efficiency and overall building performance.

This comprehensive framework evaluates a building's adaptability across various dimensions, including technical building systems, external environments, and occupant demands. It goes beyond a simple assessment, delving into three key smart functionalities: 1) optimizing energy efficiency and overall in-use performance, 2) adapting operations to meet occupant needs, and 3) responding to signals from the grid, encompassing elements like energy flexibility.

The SRI plays a crucial role in raising awareness about the manifold benefits of smart building technologies, such as building automation and electronic monitoring of heating, hot water, ventilation, and lighting systems. By implementing the SRI framework, the construction sector is incentivized to integrate cutting-edge smart technologies, fostering innovation and technological advancement.

Utilizing a "smart-ready service catalogue", the SRI categorizes building services into nine technical domains, covering heating, cooling, lighting, and monitoring. These services, defined in a technology-neutral manner, are assessed against desired impacts like energy efficiency, maintenance prediction, comfort, convenience, health and well-being, accessibility, information dissemination to occupants, and energy flexibility and storage.

The culmination of this rigorous assessment is reflected in the SRI rating—an overall score expressed as a percentage, indicating a building's proximity to maximum smart readiness. Additionally, specific scores are derived for each of the three key functionalities, providing a nuanced understanding of a building's smartness.

In essence, the SRI stands as a comprehensive framework, not just for evaluation but also for effective communication of a building's preparedness for the smart era. It underscores the integration of advanced technologies, promising heightened operational efficiency, occupant comfort, and overall building performance.

SRI and flexibility in the context of energy systems serve distinct purposes. On the one hand, SRI primarily assesses a building's capability to utilize information and communication technologies, adapt to occupant needs, and respond to grid signals, focusing on energy efficiency and overall in-use performance. It provides an overall rating and specific scores for key functionalities. On the other hand, flexibility in energy systems, particularly the FF and FI, pertains to the dynamic adjustments that buildings can make in response to external constraints or costs linked to energy use. It involves understanding how penalties influence a system's behaviour and optimize energy use patterns to minimize these penalties. In essence, while SRI evaluates a building's holistic readiness for smart technologies, flexibility explores the dynamic response mechanisms within energy systems, emphasizing adaptability to external factors and efficient energy use.

3. FLEXIBILITY FUNCION AND FLEXIBILITY INDEX

Flexibility encompasses how energy systems adapt to ever-changing demands and conditions, aiming for more efficient and sustainable energy utilization. To quantify and comprehend this concept, we introduce two pivotal notions: the Flexibility Function (FF) and the Flexibility Index (FI) [1]. These concepts aid in describing and assessing the response of buildings, systems, or devices to external signals, such as energy prices, carbon emissions, and more importantly, their energy adaptability under diverse circumstances.

The FF serves as a dynamic tool for elucidating the interplay between a penalty signal (λ_t) – representing external constraints or costs linked to energy use – and a system's responsive behavior. This is particularly relevant in the context of adaptable energy loads, such as heating systems. The process commences with the penalty generator (controller), responsible for generating penalty signals, including cost efficiency, emission efficiency, and energy efficiency. These penalty signals are derived from a multitude of factors, ranging from voltage control to load balancing, congestion management, and so on. They are then transmitted to the flexible user, whether it's a building or an energy system. The flexible user, equipped with a smart controller, interprets these penalty signals, and utilizes the information to adjust its energy use patterns dynamically as shown in Figure 1.
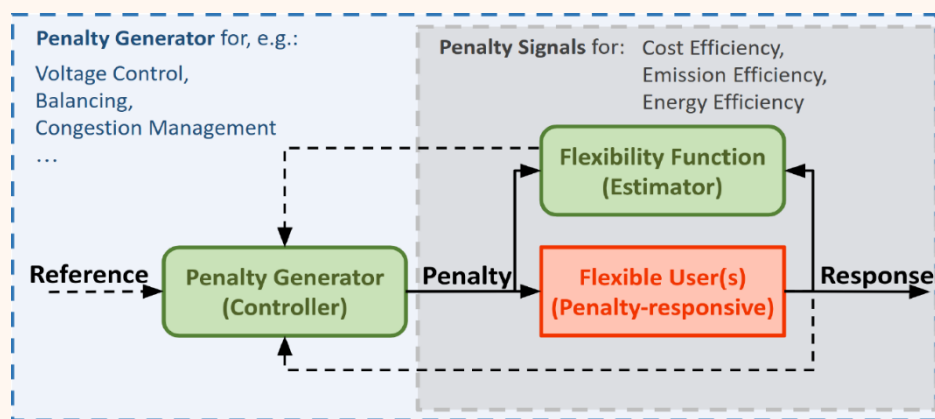

Figure 1. Flexible users and penalty signals

In essence, the FF is a dynamic analytical tool tailored to quantify and describe the energy flexibility of a given system or entity. It excels in capturing the evolving nature of energy flexibility, accommodating variations in energy demand and environmental conditions. This versatility extends to scenarios where the system is not operating under steady-state conditions. Importantly, the FF calculation does not necessitate establishing a baseline load; it can be ascertained through simulation or time series data analysis. Its broad applicability enables comparisons between systems with disparate characteristics, facilitating the calculation of total flexibility when multiple systems are combined. Furthermore, the FF methodology lends support to the provision of ancillary services to energy systems and grids, rendering it an invaluable asset for optimizing energy management and grid operations.

The Flexibility Index (FI) is a metric designed to quantify the energy flexibility of a building or system. It is defined based on the relationship between external penalty signals, such as real-time electricity prices or carbon dioxide (CO_2) costs, and the system's response to these signals. When the FI is zero (FI = 0), it indicates that the system is incapable of responding to external penalty signals. Conversely, when the FI is one (FI = 1), it signifies that the system can fully adapt to external penalty signals, minimizing associated costs or constraints to the greatest extent.

The calculation of the FI considers the system's dynamic response behavior, making it a valuable tool for assessing the system's adaptability to variations in energy demand over different time intervals. The distinctive feature of the FI is its association with reference penalty signals, which are designed to test specific system characteristics. Consequently, the FI enables the evaluation of the system's flexibility,

particularly in response to external penalties, making it a valuable tool for energy management and optimization.

The FI uses the reference penalty signal, λ, and consists of the following steps:
1. Let λt be the penalty on the energy use at time t.
2. Simulate the control of the building without considering the penalty, and let u_t^0 be the energy use at time t.
3. Simulate the control of the building considering the penalty, and let u_t^1 be the energy use at time t.
4. The total operational cost of the penalty-ignorant control is given by $C^0 = \sum_{t=0}^{N} \lambda_t u_t^0$.
5. Similarly the operational cost of the penalty-aware control is given by $C^1 = \sum_{t=0}^{N} \lambda_t u_t^1$.
6. Then the quantity $FI = 1 - \frac{C^1}{C^0}$.

In the following text, different types of the FF will be introduced, followed by need for forecasting, and characterization of the energy flexibility.

3.1. LINEAR FLEXIBILITY FUNCTION

The FF is constructed with the assumption that the system exhibits linear and time-invariant behavior, enabling it to model the system's dynamic response over time. At a specific point in time t, the system's response Y_t to the penalty signal is articulated as a convolution sum, encompassing the cumulative impact of penalties over time as:

$$Y_t = \sum_{k=0}^{\infty} h_k \, \lambda_{t-k} + R_t \tag{1}$$

where λt is the penalty signal, and Rt is the non-responsive use. The function hk is called the impulse response function.

The FF, defined as the step response function, encapsulates fundamental characteristics of the system's flexibility, by finding the expectation at time t when λk = 0 for k < 0 and λk = 1 for k ⩾ 0:

$$FF(t) = \sum_{k=0}^{\infty} h_k \tag{2}$$

It elucidates how the system adapts to changes in the penalty signal over time, encompassing the speed and extent of its adjustments to minimize associated costs or constraints.

3.2. NONLINEAR FLEXIBILITY FUNCTION

Linear FF, introduced before, provides a simplified relationship between the penalty and demand. This allows us to have a proper insight into the dynamics and introduces some features of transient and steady state demand in response to the step penalty change. However, a more realistic, and consequently, more complicated, model is required to mimic this relationship. To this end, a nonlinear FF is proposed in [2] that provides a reliable nonlinear dynamic for the demand and penalty correspondence.

The nonlinear dynamic model for the flexibility function, proposed in [2], is given as

$$dX_t = \frac{1}{C}(D_t - B_t)dt + X_t(1 - X_t)\sigma_X dW_t, \tag{3}$$
$$\delta_t = \ell(f(X_t, \alpha) + g(u_t, \beta), k), \tag{4}$$
$$D_t = B_t + \delta_t \Delta(\mathbb{1}(\delta_t > 0)(1 - B_t) + \mathbb{1}(\delta_t < 0)B_t), \tag{5}$$
$$Y_t = D_t + \sigma_Y \epsilon_t, \tag{6}$$

where X is the state of charge, B is the baseline demand, u is the energy price, δ is the demand change, D is the expected demand, Y is the observed demand, W is a Wiener process, ϵ is a random variable with

standard normal distribution, and $\mathbb{1}(.)$ is the indicator function. The other parameters can be interpreted as: amount of flexible energy (C), proportion of flexible demand (Δ), energy flexibility eagerness (k), demand with respect to the state of charge (f), demand with respect to price (g), process noise intensity (σ_X), and measurement noise (σ_Y). Moreover,

$$g(u, \beta) = \beta_1 Is_1(u) + \cdots + \beta_7 Is_7(u), \tag{7}$$

$$f(X, \alpha) = \left(1 - 2X + \alpha_1(1 - (2X - 1)^2)\right)(\alpha_2 + \alpha_3(2X - 1)^2 + \alpha_4(2X - 1)^6), \tag{8}$$

$$\ell(X, u, k) = -1 + \frac{2}{1 + e^{-k(f(X) + g(u))}}, \tag{9}$$

with $\alpha_i, i = 1, \dots, 4$, and $\beta_j, j = 1, \dots, 7$, to be identified and Is_i are I-spline functions [2]. Equations (3)-(5) along with (6)-(8) construct a nonlinear price-demand mapping. In this system, X plays the role of the state of charge, that is, $X = 0$ implies that energy use cannot be reduced further and $X = 1$ implies that there is no room for more energy use. Considering Equation (3), the state of charge increases if demand surpasses the baseline, and vice versa. Also, the term $X_t(1 - X_t)$ ensures that the noise term becomes zero as X_t meets its upper or lower bounds. The parameters of this grey-box model can then be estimated by maximizing the likelihood function [3, 4].

3.3. ADAPTIVE FELXIBILITY FUNCTION

The dynamics of a given energy system changes over time due to gradual deterioration, seasonal changes (e.g., in ambient temperature), consumer behaviour (e.g., during holidays), etc. Therefore, the dynamics of the price-demand relationship changes as well. This motivates the design of a mechanism that accounts for such dynamic variations [5]. The issue of parametric uncertainty can be mitigated using either passive or active approaches. Passive methods are based on robust fixed-structure control systems considering bounded parametric uncertainty. In contrast, active methods are based on adaptive control methods that adjust the control law based on the changes in system parameters.

The adaptive penalty signal should be calculated by using:

$$u_t = \hat{\alpha}_t X_t + \hat{\beta}_t r_t + \hat{\zeta}_t, \tag{10}$$

where the adaptive parameters $\hat{\alpha}$, $\hat{\beta}$ and $\hat{\zeta}$ are calculated by solving the following differential equations:

$$\dot{\hat{\alpha}} = \gamma_\alpha \, Proj(\hat{\alpha}, Xe), \tag{11}$$

$$\dot{\hat{\beta}} = \gamma_\beta \, Proj(\hat{\beta}, re), \tag{12}$$

$$\dot{\hat{\zeta}} = \gamma_\zeta \, Proj(\hat{\zeta}, e), \tag{13}$$

where the projection operator [6, 7], $Proj$, is employed to keep the parameters of the adaptive system bounded, and X is calculated by using:

$$X = \int_0^t \frac{1}{C}(D_t - B_t)dt, \tag{14}$$

where C is the capacity of the flexible energy, D is the expected demand, B is the baseline demand and $r = D_{ref} - B$, where D_{ref} is the reference demand. When e is calculated as $e = X - Y$, Y can be obtained as:

$$\dot{Y} = \lambda Y + \frac{1}{C}r. \tag{15}$$

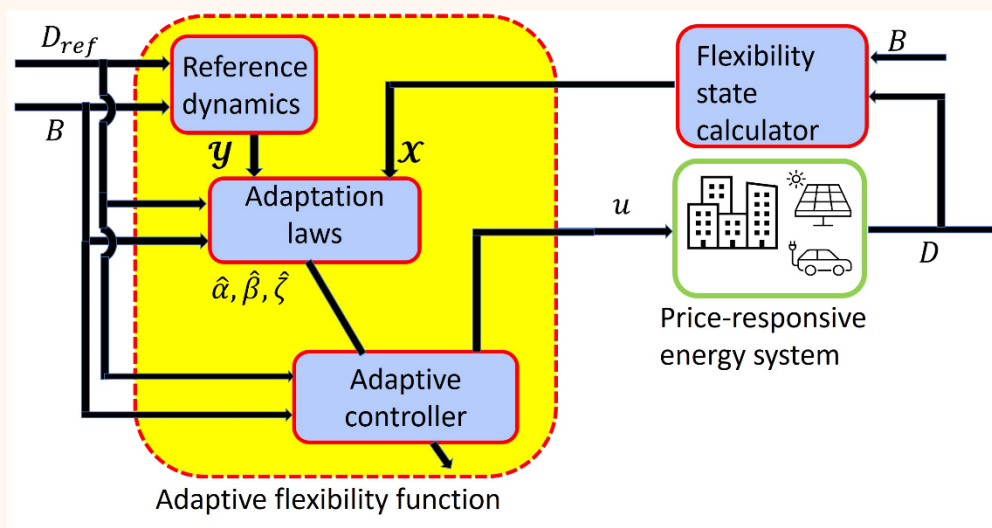The block diagram of the adaptive FF is given in Figure 2.

Figure 2. Block diagram of the adaptive flexibility function.

3.4. LEARNING FROM DATA AND NEED FOR FORECASTING

The FF and FI are not static concepts but rather dynamic tools that evolve with data-driven insights. Through continuous data collection and analysis, these metrics gain a deeper understanding of a system's behaviour over time. For instance, by examining historical data on energy use patterns, a FF can adapt to recognize recurrent trends, seasonal variations, and specific operational nuances. This learning process allows the FF to become increasingly accurate in predicting and responding to penalty signals.

Forecasting is another integral aspect of the utilization of the FF and FI. These tools leverage forecasting models to anticipate future energy demands, penalty signals, and system responses. By integrating forecasting techniques, FF and FI can pre-emptively adjust a system's energy use patterns to optimize cost savings and minimize environmental impacts. For example, in the context of renewable energy sources like solar and wind, forecasting helps predict energy availability, allowing the system to proactively shift use to periods of abundant renewable generation. Incorporating learning from data and forecasting capabilities into the FF and FI enhances their ability to provide real-time, data-driven insights. This empowers energy systems to not only react to immediate penalty signals but also to proactively plan and adapt to changing conditions, ultimately contributing to improved energy efficiency, cost savings, and sustainability.

3.5. CHARACTERIZING THE ENERGY FLEXIBILITY

Figure 3 provides an illustrative example of how buildings respond when receiving a penalty signal and the parameters that characterize the response to this signal. It is essential to recognize that a building's energy flexibility is not a fixed, static value but rather a dynamic parameter influenced by various factors. These factors include environmental conditions, occupant behavior, and the specific characteristics of the penalty signal, which triggers a system response. Consequently, a building's energy flexibility is determined by its capacity to adjust its instantaneous energy demand strategically, aiming to minimize the impact of the penalty signal. The penalty signal itself can be tailored to achieve multiple objectives, such as 1) reducing energy use, 2) minimizing costs, 3) decreasing the building's CO_2 footprint, or a combination of these criteria.
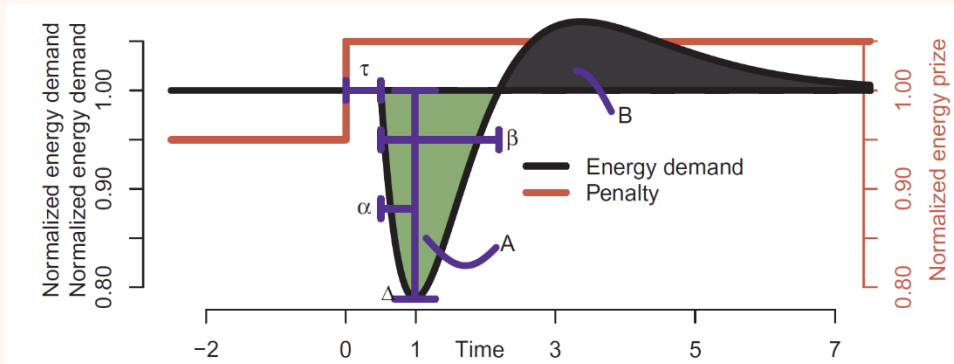
Figure 3. Example of aggregated response when some buildings receive a penalty signal – here a price signal. τ (Time): The delay from adjusting the energy price and seeing an effect on the energy demand. 0.5 in the example. Δ (Power): The maximum change in demand following the penalty change. α (Time): The time it takes from the start in change in demand until it reaches the lowest level. 0.6 in the example. β (Time): The total time of decreased energy demand. 2 in the example. A (Energy): The total amount of decreased energy demand. B (Energy): The total amount of increased energy demand.

The Penalty signal can take on two distinct forms:
  – Step Response: This variant of the signal involves a sudden and drastic change, similar to a rapid shift in energy prices, as illustrated in Figure 3. It is employed to evaluate various facets of the energy flexibility accessible within a building or a group of buildings.
  – Temporal Signal: In contrast, the signal may exhibit temporal variations over the course of a day and throughout the year. These variations align with the demands and conditions of the energy networks, as exemplified in Figure 4. This type of signal reflects the dynamic nature of energy requirements and network constraints.

The step response test serves multiple purposes, including its application in simulations to assess the thermal storage system's capabilities. Additionally, it can be implemented in real energy networks for peak shaving operations. The temporal signals find extensive usage when harnessing energy flexibility within a specific segment of an energy network. These signals provide valuable insights into the available energy flexibility in that specific context.

3.6. EXAMPLE OF BUILDING FLEXIBILITY

Consider a common scenario involving a building that requires heating, with the penalty signal representing the energy price. In this context, the penalty-aware controller's objective is to maintain the building's temperature within predefined thermal comfort limits while minimizing overall heating costs. This concept is effectively illustrated in Figure 4, which provides a graphical representation of the process. The top plot visualizes the temperature within a building under the control of two distinct controllers: a penalty-aware controller focused on cost minimization (depicted in green and dashed lines) and a conventional controller primarily focused on energy consumption reduction (represented in red and solid lines). Moving to the middle plot, we observe the penalty signals (represented as black columns) and the corresponding heating operations performed by both controllers. Notably, the regular controller tends to maintain the temperature slightly above the minimum required level, as shown in the general trend. Opposite, the penalty-aware controller exhibits a more dynamic behavior, heating the building during periods of lower penalties, resulting in higher temperature variation. The lower plot provides insights into the accumulated penalties for each controller. As anticipated, the regular controller accumulates a higher penalty compared to the penalty-aware controller. This core concept of penalty-aware control may be adaptable to a wide range of flexible systems and various penalty signals.
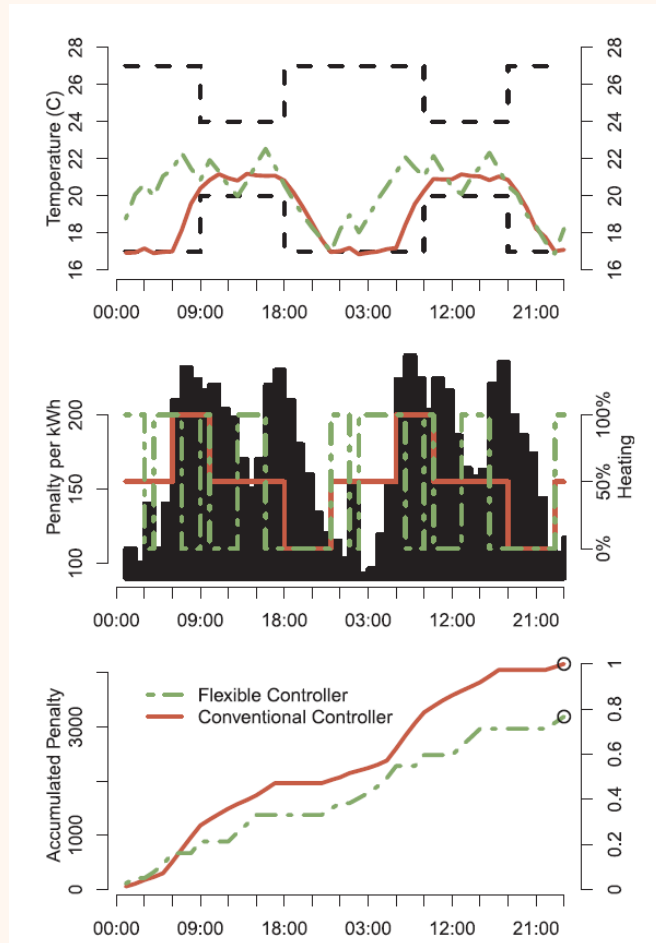
Figure 4. Top plot: An example of the temperature in a building controlled by a penalty-aware controller (green, dashed) and a conventional controller (red, solid). Both controllers are restricted to stay within the dashed lines. Middle plot: The black shading gives the penalties, while the green and red lines show when the two controllers heat, respectively. Bottom plot: These graphs illustrate the accumulated penalty for each of the controllers.

4. FLEXIBILITY POTENTIAL IN BUILDINGS

In this section, examples of using flexibility potential of the buildings are provided. This potential exists due to the thermal capacity of the building, the storage tanks, district heating, and batteries. Seven different case studies are investigated and presented in the text below. For each case, basic demo descriptions are given first and then possibility for utilizing energy flexibility are explained.

4.1. CASE STUDY: SØNDERBORG, DENMARK

The Sønderborg demo case is called SAB22 and comprises of 19 multi-family buildings. These buildings were constructed in the 1970s but have been renovated frequently. Each building has a similar floor plan and the only differences between them are their orientation, floor area and number of floors. Figure 5 depicts an aerial view of the demo case, as well as a photo of one of the blocks.
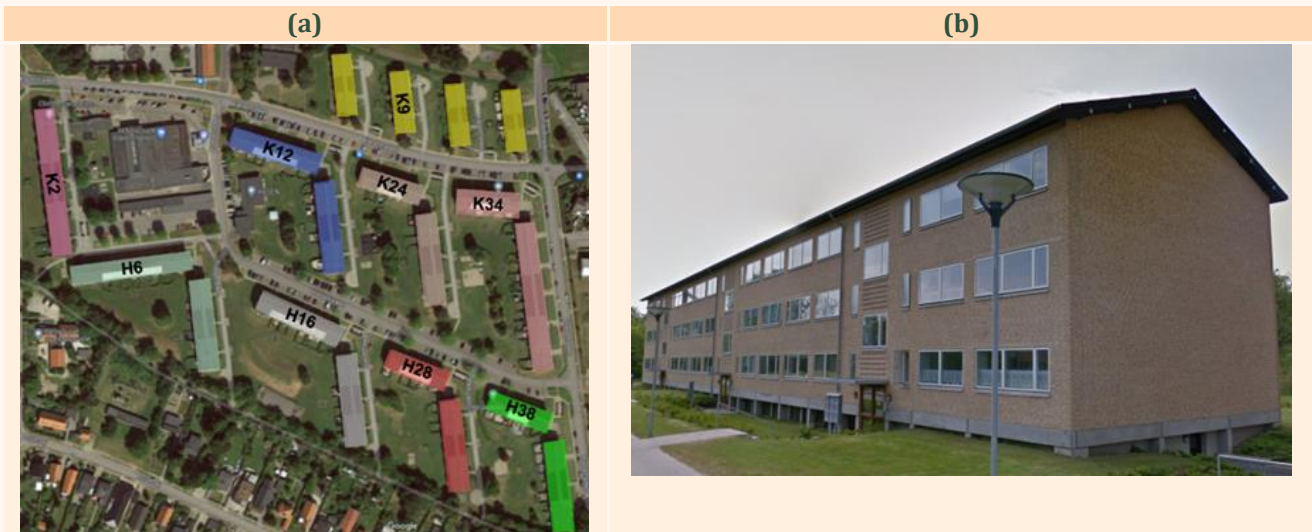
(a)	(b)

Figure 5. (a) Arial view of the neighborhood and district heating substations in Sønderborg. Colors represent individual substations. (b) Photo taken from one of the buildings of SAB22

The heating demand in the area is satisfied by a nearby district heating plant. There are nine substations that distribute heat to 19 building blocks. Each of the substations is labelled to its corresponding block. The exact information about the building construction elements was not available. Therefore, valid datasets were used to gather this information. These datasets include the Danish Building and Housing Register (BBR) [8], Danish building standard (DS/EN 15251) [9], and the TABULA project [10]. The components of the buildings that were considered in the building models are listed in Table 1.

Table 1. Components used in creating building models of SAB22

Component	Materials (thickness)
Roof	Roof tiles (59 mm) Insulation (300 mm) Hollow core concrete (270 mm)
Exterior wall	Brick (108 mm) Insulation (375 mm) Aerated concrete (100 mm)
Floor/ceiling	Concrete (220 mm) Insulation (93 mm) Concrete (80 mm) Oak planks (14 mm)
Ground floor	Insulation (350 mm) Concrete (120 mm)
Windows	Clear double glazing with air
Internal wall	Concrete (200 mm)

For the space heating, district heating supply water is mixed by the return water from the radiators (by controlling the mixing ratio) to provide a proper supply temperature for the radiators. The proper temperature is determined by a Weather Compensation Curve (WCC) that ensures a reliable heat supply to the blocks in all weather conditions. The radiators are equipped with Thermostatic Radiator Valves (TRV), automatically adjustable valves for maintaining indoor temperature at a certain range.

In the Sønderborg case, the space heating system has been chosen for analysis and calculation of its flexibility. The indoor temperature is used as a direct indicator of the heat use in buildings, which can be flexibly changed within the comfort range. To achieve this, a suitable controller is required to control the components. Price-responsive controllers are simple and efficient controllers that can unlock the energy flexibility of systems. Therefore, a simple rule-based controller has been considered for the Sønderborg case, which can directly control the indoor temperature by changing TRV setpoints. The indoor temperature is assumed to change between 18°C and 26°C according to the price. However, to ensure that high setpoints are reachable, and to prevent high return water temperatures at low setpoints, the forward temperature of radiators should also be controlled. Therefore, it is also considered to change according to the setpoint and ambient temperature, as shown in Figure 6.
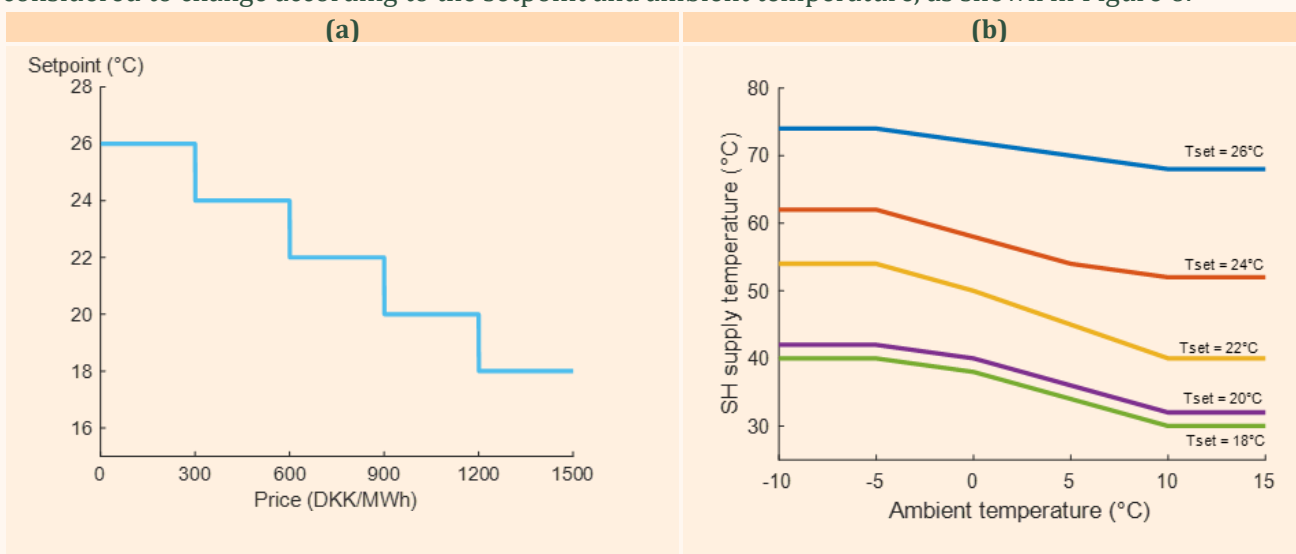

Figure 6. (a) Indoor setpoint control based on the heating price. (b) Space heating supply temperature as a function of indoor setpoint and ambient temperature.

Baseline power, observed power, and applied heating price data for a specific period are needed to determine the parameters of the flexibility function for the neighbourhood. An iterative method is used to fit the model to the data and calculate the parameters. For this purpose, a one-month period in February 2022 has been chosen. As the heating cost is currently fixed in Denmark, dynamic electricity price from Nordpool Day-ahead market for DK1 was taken as the heating cost. Simulations were conducted using the white-box Modelica model and present the results in Figure 7.
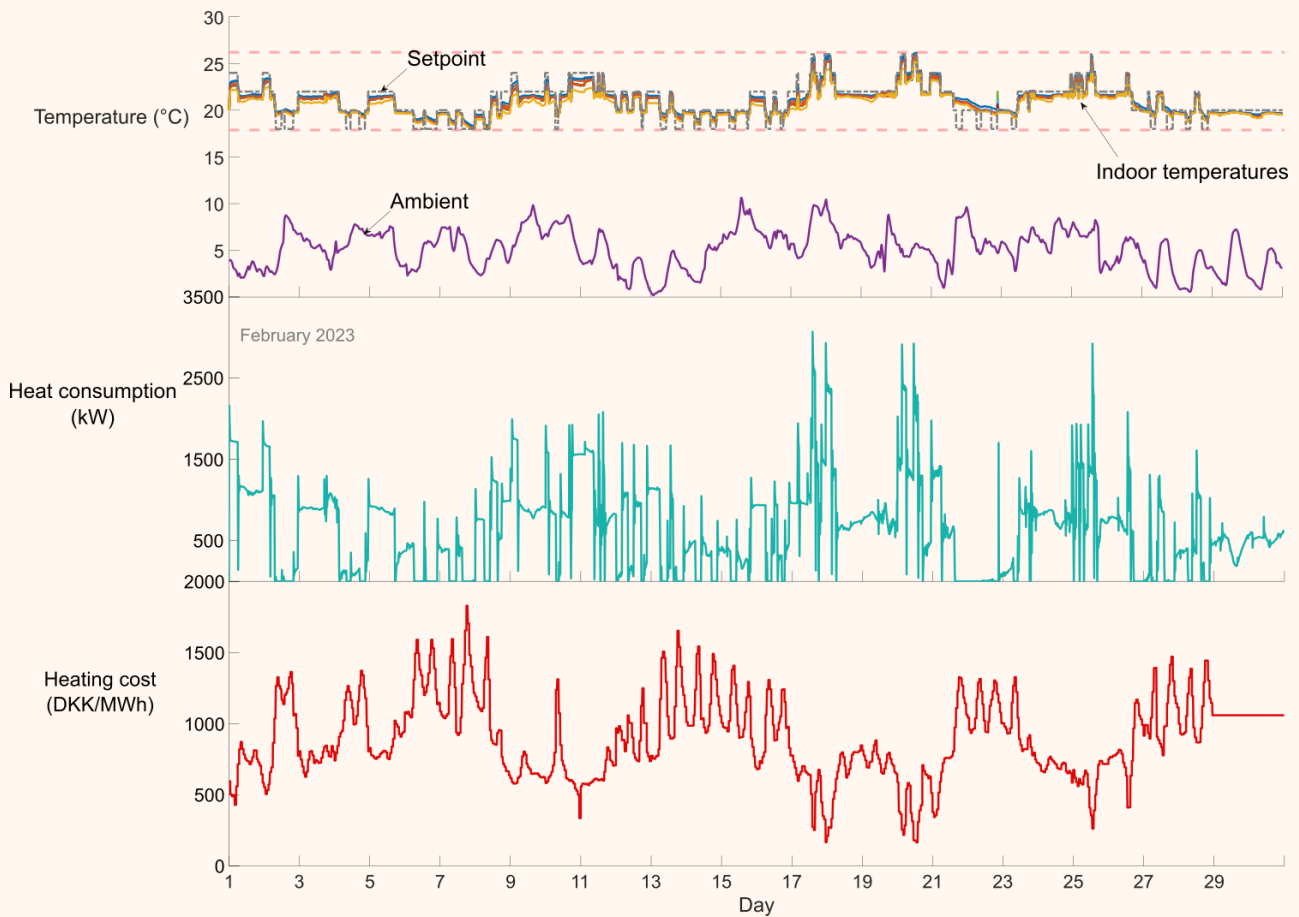
Figure 7. Results of applying dynamic heating cost to the buildings with price-responsive controllers. (Top) indoor temperatures together with ambient temperature, (middle) total space heating consumption of the neighborhood and (bottom) the heating cost taken from Nordpool DK1 day-ahead electricity price.

The indoor setpoints, determined based on the heating cost, are represented by a dashed line on the top. The indoor temperatures were found to successfully follow the setpoints. However, when the setpoint drops to the lowest value, the indoor temperatures take more time to reach the setpoint, due to the thermal lag of the buildings (for instance, days 21-23). This is good news as it indicates that the heating system can be turned off during high price periods, and the flexibility is being utilized effectively. Additionally, the total space heating use profile shows a strong correlation with the heating cost. For example, drops in the heating cost on days 18 and 20 are followed by spikes in heat use during the same periods.

To determine the baseline demand, the system was tested under the same conditions but with normal controllers that have fixed TRV settings of 22°C, instead of price-responsive controllers. The resulting data was then used to estimate the parameters of the nonlinear flexibility function, which are listed in Table 2.

Table 2 Parameter estimates of the flexibility function model for the neighborhood.

Parameters	values
Δ	1
C	4.659363
α_1	-0.068133
α_2	0.210158
α_3	0.181272
α_4	0.607677
K	1.581067
x_0	0.263674

log(sY)	-1.85215
β_1	0.103038
β_2	0.292141
β_3	0.142494
β_4	0.158005
β_5	0.306071
β_6	0
β_7	0
lambda	16.5031

4.2. CASE STUDY: FREDRIKSTAD, NORWAY

A Norwegian case is part of a new development in Fredrikstad, called Verksbyen, representing the subarctic European climate, see Figure 8. Please note that this case is not a part of the ARV project, but the example is relevant to show energy flexibility. The case is the largest development of plus energy houses in Norway, and it has a strong focus on energy sharing and flexibility in the neighbourhood. The demonstration case will be built in Fredrikstad, which is a town located approximately 90 km south of Oslo. The total development consists of more than 1 500 dwellings, a kindergarten, a school, and commercial buildings [11].

Figure 8. Illustrations of the Verksbyen demonstration project in Fredrikstad, Norway.

The idea of the project in Fredrikstad is that HVAC system of the entire neighbourhood will be controlled by an advanced controller. The energy system of the area consists of a heat pump, generating the required thermal demand, and a storage tank that provides the required domestic hot water for the building. A model predictive controller (MPC) has been developed to shift the demand based on some predefined penalty signal. The designed controller is also able to take into account the technical constraints and future predictions. The efficiency of the employed controller is demonstrated in Figure 9. The top panel shows the water temperature of two layers of the tank. The second panel shows the electricity use to increase the water temperature in the tank. The ambient temperature is provided in the third panel. Requested load of each tank and the penalty signal are shown in the fourth and fifth panels, respectively. It is observed that the controller shifts the demand to the periods of time when the electricity price is lower.

The designed controller's (with variable penalty) performance can be compared to a controller which is not affected by a penalty signal (constant penalty). Figure 10 demonstrates the accumulated energy and penalty with constant and variable penalty signals. Figure 10 shows when using time varying penalty signal, the accumulated energy is higher, by about 1%, compared to using the constant penalty signal. However, the bottom panel demonstrates that the accumulated penalty is dramatically higher, by 60%, when the constant penalty signal is employed. This means that MPC can handle energy use while reducing the electricity costs. Flexibility index for the short term (a week during the winter) and long term (the whole year) are 66.44% and 67.7%, respectively, indicating high flexibility of the system induced by MPC and water storing tank implementation.
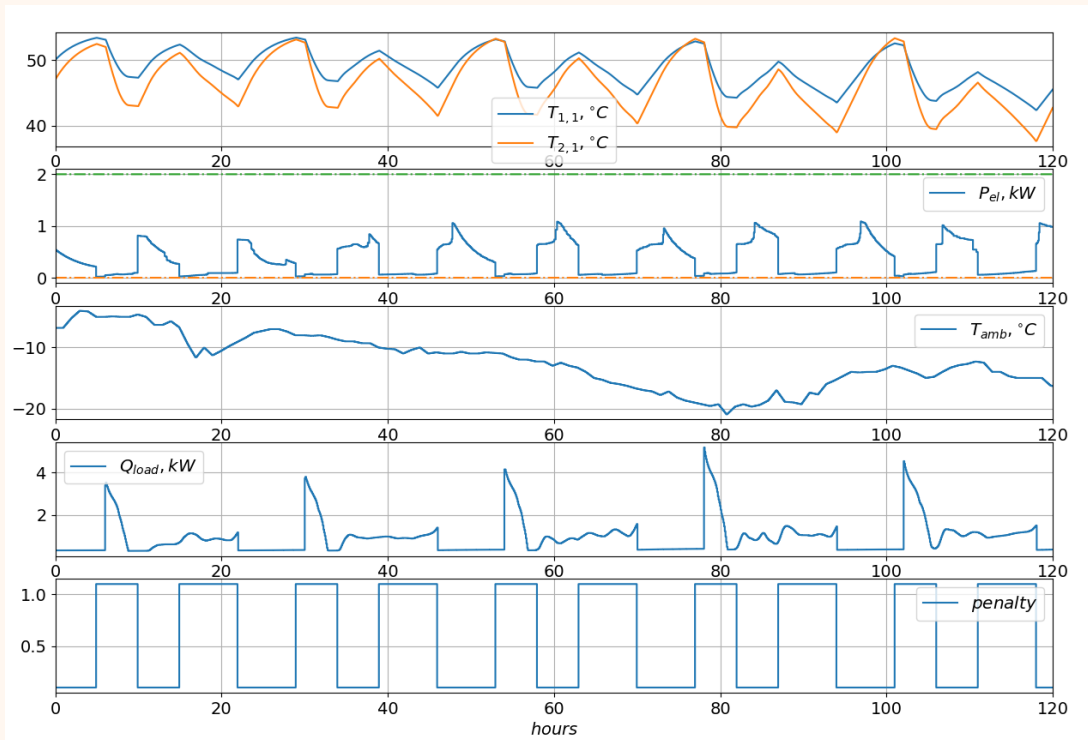

Figure 9. Simulation results of MPC using variable penalty signal. The top panel shows the water temperature of two layers of the tank. The second panel demonstrated the electricity consumption to control the water temperature of tank. The ambient temperature is provided in the third panel. Requested load of the tank and the penalty signal are shown in the fourth and fifth panels, respectively.
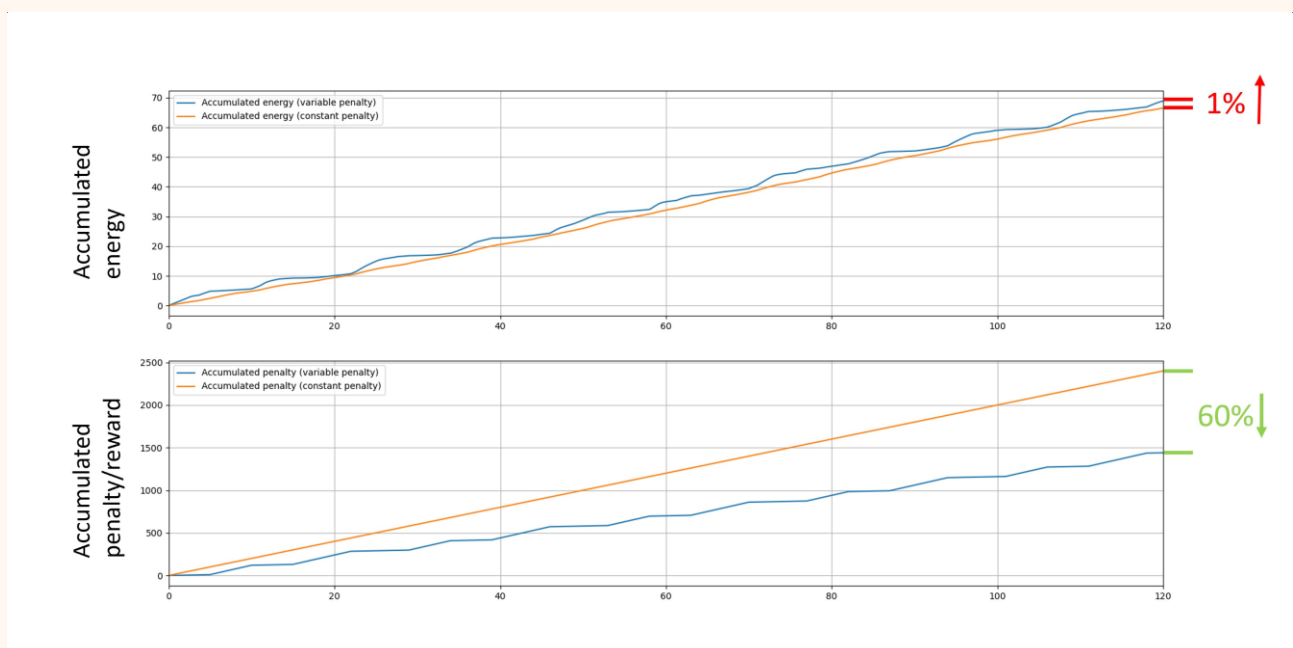

Figure 10. Accumulated energy and penalty.

The above results show the flexibility potential of the Fredrikstad neighbourhood, and the capability of the MPC to extract it. However, the results do not consider the higher levels of the smart energy operating systems. There are many players in the modern energy systems like DSOs, TSOs, electricity markets and aggregators that should be considered. Aggregators are in connection with the DSO, TSO, market, and the consumers. Furthermore, they buy an amount of energy for each hour of the day based on the forecasts, baseline demands, and other parameters. Once the bought energy is determined, a smart scheduling algorithm is required to manage use. This can be done using an economic MPC that requires price signals.

A dynamic price-demand mapping, like the FF, is required to connect the physical level to the market level in the smart energy operating system. The parameters of a nonlinear FF are being identified and the results show that the FF can predict well the demand, see Figure 11.
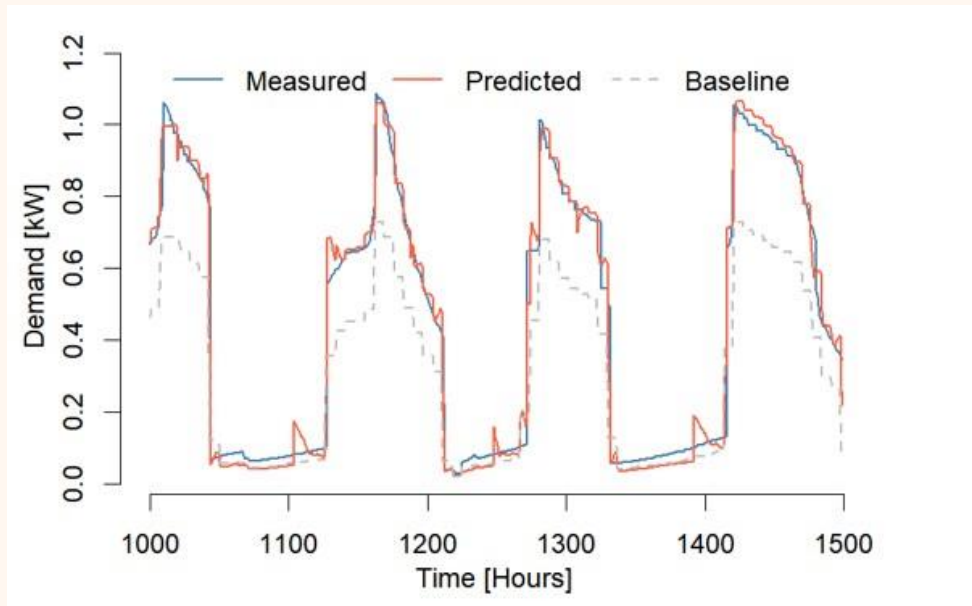

Figure 11. Measured and predicted demand using flexibility function

The identified FF provides an invaluable information to find an optimal penalty signal for the MPC. The optimal penalty can be generated by minimizing the difference between the predicted demand, as the output of the FF, and the reference demand, provided by the aggregator:

$$arg \min_{u} \sum_{k=1}^{m} \left(D_k(B, u) - D_{ref_k} \right)^2 , \qquad (16)$$

where D_{ref} is the bought energy and can be considered as a reference to be followed, D is the predicted demand by the FF. Figure 12 illustrates the price signal (U) with response to the bought energy (D_{ref}). It is seen that the price signal is generated such that the difference between demand (D) and the bought energy (D_{ref}) is minimized. This is done by solving the optimization problem in Equation 16. The generated price signal should then be implemented in the MPC to control the HVAC system of the observed case [11]. An economic MPC has been designed with the cost function $\sum_{j=0}^{N-1}(U \times P_{el})$, where N is the control horizon, U is the penalty signal, penalizing when the electricity price is high, and P_{el} is the electricity use. Simulation results of the economic MPC using the generated price signals are given in Figure 13. The top panel of Figure 13 shows the water temperature of two layers of the storage tank ($T_{1,1}, T_{2,1}$). The second panel shows the electricity use to increase the water temperature of the tank. The ambient temperature is provided in the third panel. Load and the penalty signal are shown in the fourth and fifth panels, respectively.
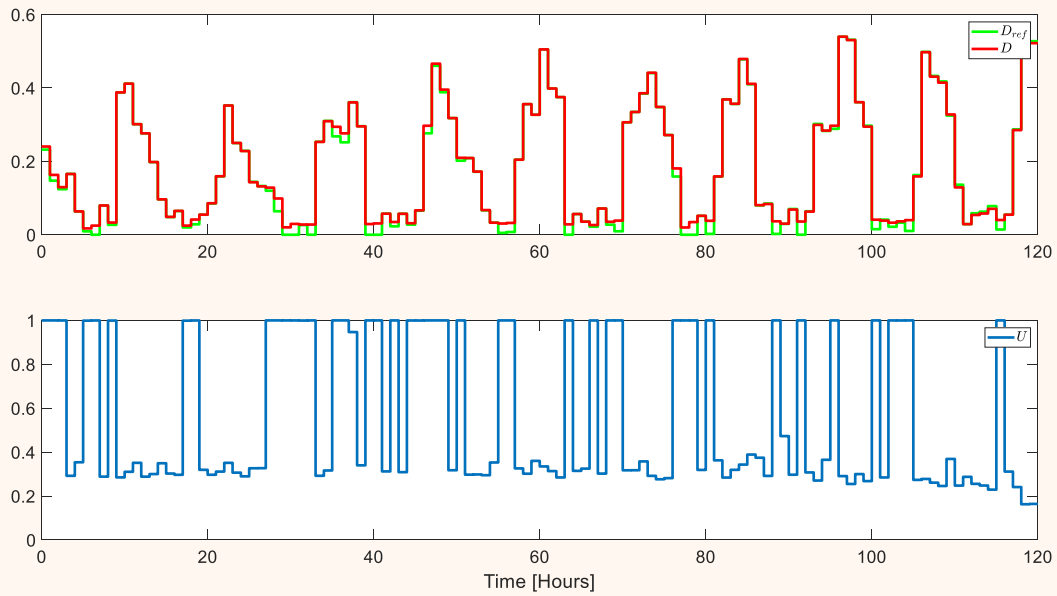
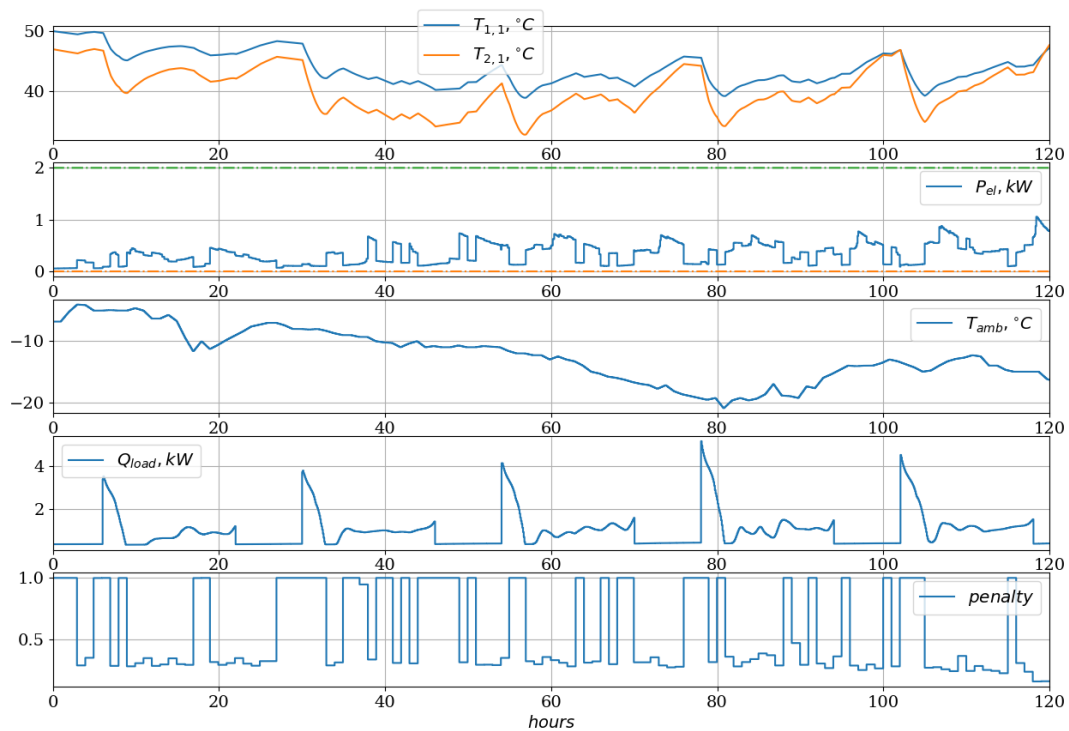*Figure 12. Price signal generation using flexibility function.*

Figure 13. Model predictive control results using the generated penalty signal. The top panel shows the water temperature of two layers of the tank. The second panel demonstrated the electricity consumption to control the water temperature of tank. The ambient temperature is provided in the third panel. Requested load of the tank and the optimal penalty signal are shown in the fourth and fifth panels, respectively.

4.3. CASE STUDY: COPENHAGEN, DENMARK

HOFOR (district heating utility in Copenhagen), Copenhagen City Properties & Procurement (Municipality's building department) and Danfoss have tested the potential of minimizing peak heating demand to increase usage of CO_2 neutral base-load heat production in Copenhagen, by utilizing Leanheat Building AI-based heating control.

The first part of the demonstration took place in the heating season 2021/2022 and included 17 municipal buildings (mainly daycare centers). The buildings were already equipped with the Danfoss ECL310 heating controller and they were connected to the Leanheat AI control via the Danfoss ECL portal.

The main goal of the demonstration was to reduce the peak in heat demand that occurs in the mornings (6-10 am) by making the heat use more flexible. Thus, the project has been named district heating Flexumers, since the buildings that previously were only seen as energy users, become an active part of the district heating system. Each building acts as a virtual heat plant by increasing its use when heat production is cheap and ecological, and decreasing during times of high demand, by providing flexibility on the consumption side.

Leanheat's AI learns how the building thermal mass reacts to the ambient conditions and evaluates the flexibility potential based on the forecasted weather and set comfort requirements. The estimated flexibility can then be used by the district heating utility to minimize the load during peak load periods. As an example, during the morning peak, the control allows the discharging of the heat previously stored in the buildings by reducing the supply temperature for space heating up to 30%, after which it is recharged as soon as possible, and anyhow before the next morning. The variation of supply temperature during this period still ensures that the thermal comfort in the building stays within the recommended limits. As presented in Figure 14, the initial results of the demonstrations for the cluster of 17 buildings show that the average morning peak is decreased by 14%, compared with the average peak use before the implementation of the smart control. The connected buildings also reduced their heating energy use predictively factoring in upcoming changes in weather, such as solar radiation and wind. Due to the success of this pilot project, the plan is to upscale the numbers of involved buildings up to 700.
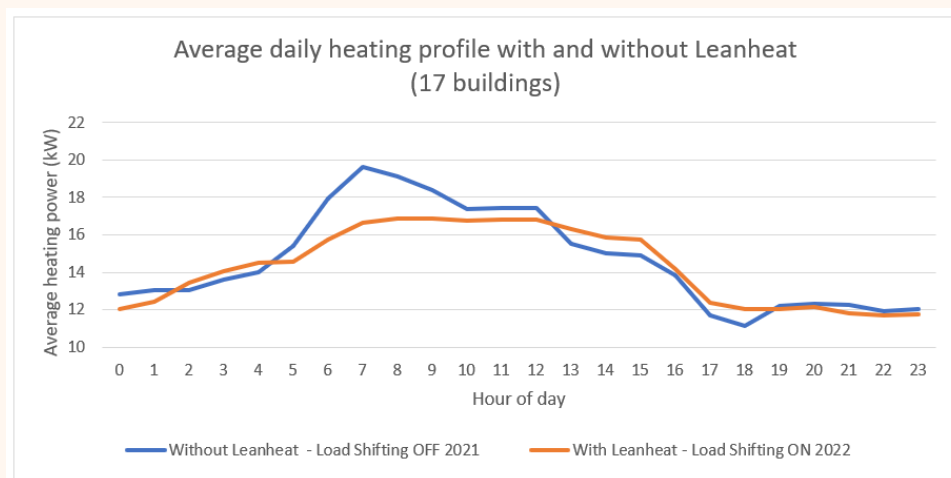

Figure 14. Average daily heating profile with and without Leanheat control.

Looking at peak demand data measured at the buildings presented in Figure 15, the maximum peak power has decreased from 27.5 kW/building to 21.5 kW/building, a reduction of 22%. The calculation is done by comparing the highest peak during load shifting to the highest measured peak in the previous heating season at the same outdoor conditions.
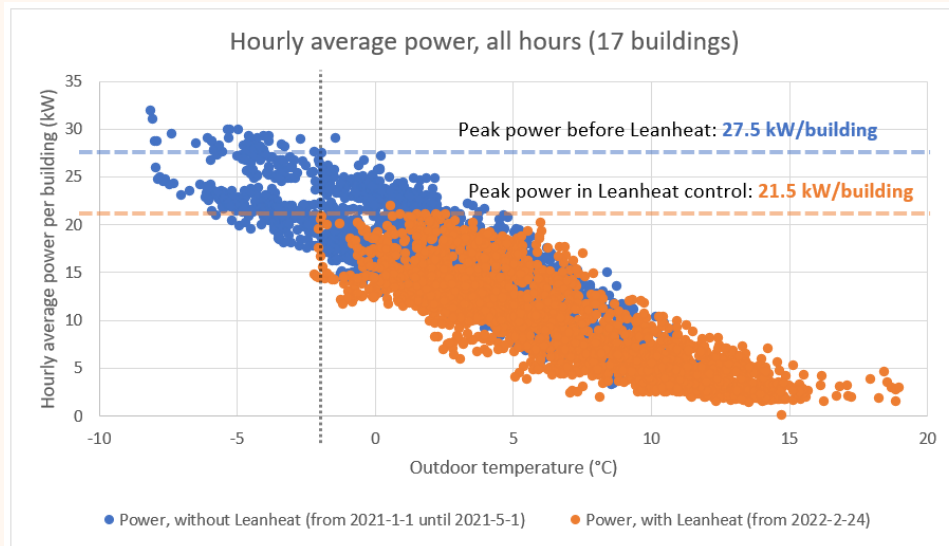
Figure 15. Hourly peak power in buildings, with and without Leanheat control.

HOFOR sees district heating Flexumers as an important measure to minimize fossil-based peak load production and incentivize renewable-based heat-producing units. In fact, the same principle of peak power optimization, about charging and discharging the thermal energy in the building mass, can be utilized in demand-response solutions for district heating, where Danfoss Leanheat can offer flexibility from an aggregated building stock, making it possible for the district heating company to produce heat and use it in the buildings when it is most beneficial economically or ecologically, reducing the use of fossil-based heat sources and prioritizing the renewable-based ones. As an example, with the advanced knowledge of the building thermal mass, Danfoss Leanheat Building can enable the use of price signals to adjust the building heat supply to take advantage of low-cost periods, for example when there is a large share of fluctuating renewable energy in the system [12].

4.4. ESTIMATION OF THE DHW LOAD SHIFT POTENTIAL, CASES IN DENMARK

DHW data from five buildings located in Kolding, Hillerød, and Copenhagen has been investigated, with the aim to estimate the load shift potential related to energy storage in building level DHW systems based on storage tanks. Based on this, the qualitative and quantitative DHW tapping profiles over the day and over the year was obtained, giving the basis for estimating the load shift potential.

To estimate the district heating (DH) load shift potential related to the service of DHW, the hourly DHW tapping energy is assumed to represent the charging load of the DHW storage tank by the DH net. A DHW storage tank model is applied to simulate to what extend the DH charging energy can be shifted outside the predefined peak load periods for the morning and the evening, without compromising the DHW supply temperature. To distinguish between seasons for DHW tapping, a low season and a high season for DHW tapping is applied as well. This season is also related to the heating season. In this way it is possible to differentiate the load shift potential during the cold season where heating is applied and the warm season. Figure 16 illustrates the basic principle of the load shift potential estimation method.
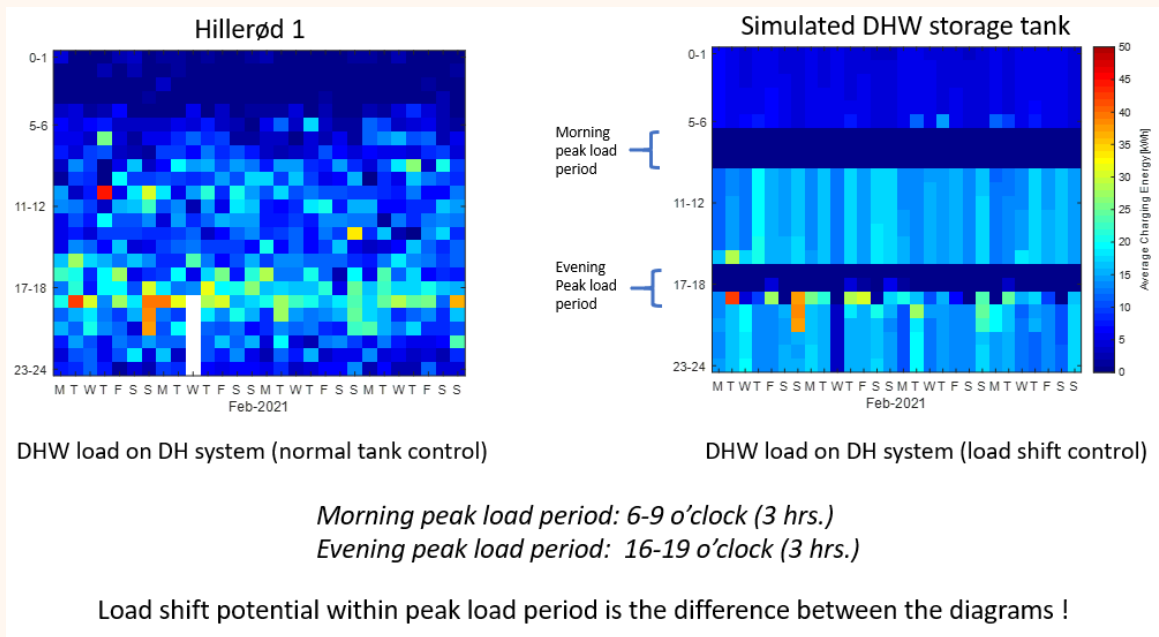
Figure 16. Illustration of the principle for estimating the load shift potential for DHW.

The example in Figure 16 shows that all DHW load can be shifted outside the defined morning peak load period. For the evening peak load period this is not the case, because there remains a load on the DH network during the end of the defined peak load period. The reason is that the DHW tapping load level during the defined peak load period, which in this case is higher for the evening peak period compared to the morning peak period.

Due to the stochastic variation of the DHW tapping from day to day, and the variation over the year, the load shift potential varies. In Figure 17, the estimated load shift potential histograms are shown for case Hillerød 1 as example. It is divided into low and high DHW season and morning and evening peak.
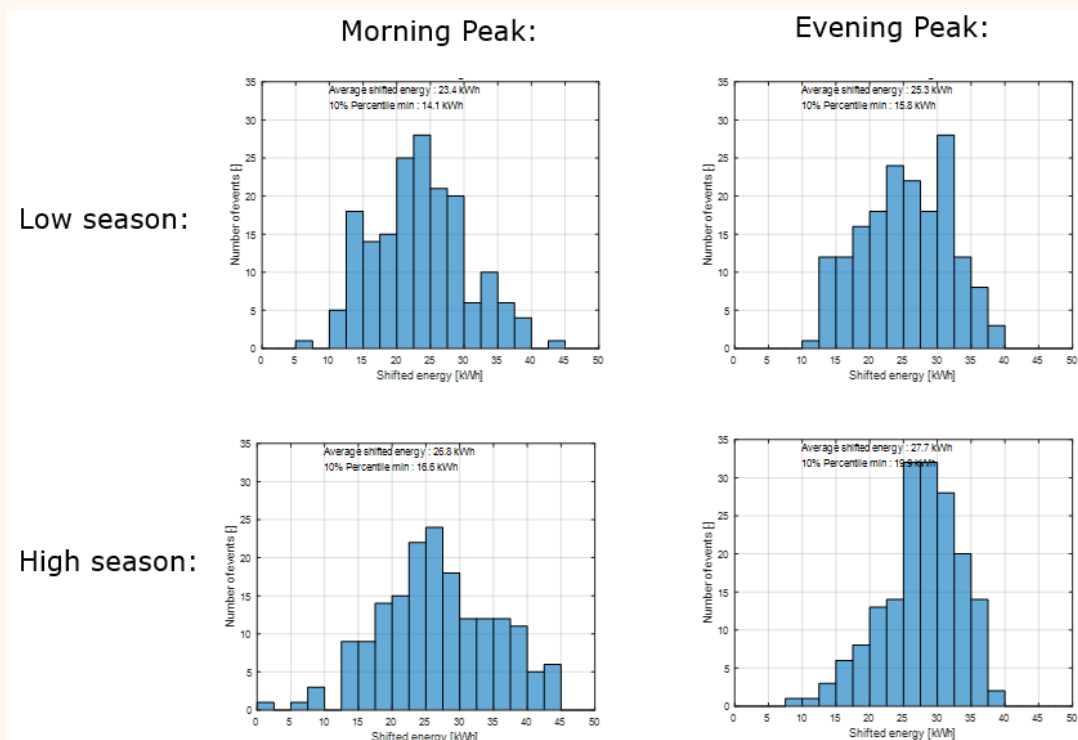

Figure 17. Potential load shift energy distribution for Hillerød 1

Due to the spread of DHW tapping, it is not straight forward to estimate the load shift potential accurately for the next day. To indicate a level for the minimum expected load shift potential, the 10%

percentile value is calculated, indicating the minimum expected load shift energy for 90% of the events. Table 3 shows, that the load shift potential (in kWh for the three hours peak period) is generally larger for the morning peak compared to the evening peak. As an average, 20% of the daily energy for preparing the DHW can be shifted away from the defined morning peak and 12-13% for the evening peak.

Table 3. Table with estimated load shift potentials

Location:	Nos. Flats	Load shift morning [kWh]	% of daily DHW energy [-]	10% Percentile, morning [kWh]	Load shift evening [kWh]	% of daily DHW energy [-]	10% Percentile, evening [kWh]	daily DHW energy [kWh]	daily DHW energy/flat [kWh]
Low Season									
Kolding 1	31	8,8	33%	5,2	2,6	10%	1,3	27	0,9
Kolding 2	47	15,5	17%	10,5	11,9	13%	7,6	89	1,9
Hillerød 1	42	23,4	14%	14,1	25,3	15%	15,8	166	4,0
Hillerød 2	30	21,1	16%	12,8	20,2	15%	11,8	133	4,4
HOFOR 3	22	15,0	22%	3,3	8,4	12%	2,0	68	3,1
Average		16,8	20%		13,7	13%			

Location:	Nos. Flats	Load shift morning [kWh]	% of daily DHW energy [-]	10% Percentile, morning [kWh]	Load shift evening [kWh]	% of daily DHW energy [-]	10% Percentile, evening [kWh]	daily DHW energy [kWh]	daily DHW energy/flat [kWh]
High Season									
Kolding 1	31	9,6	28%	5,7	3,5	10%	1,3	34	1,1
Kolding 2	47	20,2	16%	13,6	16,2	13%	11,2	126	2,7
Hillerød 1	42	26,8	12%	16,6	27,7	12%	19,9	229	5,5
Hillerød 2	30	25,8	15%	14,8	24,9	15%	16,1	170	5,7
HOFOR 3	22	27,4	30%	5,8	9,4	10%	3,6	90	4,1
Average		22,0	20%		16,3	12%			

Comparing the potential load shift energy to an average space heating capacity, it corresponds to 10-15% of the average space heating capacity during the high season or heating season. In this perspective, the load shift potential appears very relevant on an additional flexibility on top of the load shift potential originating from the heating system. When looking at the 10% percentile for all locations except HOFOR 3, then approximately 60% of the load shift potential is expected in 90% of the events. For HOFOR 3, the low value for the percentile is related to basically no tapping in weekend morning peaks and in general low tapping's in the evening peak load period and some spread tapping outside the peak periods. In this perspective the HOFOR3 is considered as an outlier. Further, DHW provides load shift potential all year around which is not the case for the load shift originating from the heating system. The finding of this case study is that the load shift potential for DHW is relevant for four out of the five locations, mainly determined by the DHW tapping level and how it time vice correlates with the defined peak load periods.

4.5. CASE STUDY: OVERVECHT NOORD AND KANALENEILAND-ZUID DISTRICT, DUTCH

The Dutch demo case focuses on flexibility functions, aiming to achieve fossil-free status by 2030 and renovate social housing in Overvecht-Noord and Kanaleneiland-Zuid districts. These districts, built in the 1960s and 1970s, have a multicultural community with social housing and low-income households relying on district heating, gas, and electricity grids.

In Overvecht-Noord, the goal is to renovate around 5 000 social housing units and achieve Zero or Positive Energy Buildings (PEB) target. This involves addressing challenges such as limited renewable energy options, space requirements, innovation, collaboration, and resident confidence in long-term energy performance.

The pilot building in the Dutch Demo plays a pivotal role in sustainability studies. One such case study is the PEB on the Henriettedreef in Utrecht, located in the Overvecht-Noord District, see Figure 18. This case study examines the renovation of a high-rise building to achieve positive energy performance.

The FF in the Dutch demo includes PV forecasting using sky imagers to forecast irradiance, enabling accurate predictions of PV output. This information is then utilized to optimize the flexibility of batteries by maximizing self-consumption and peak shaving.

Renovating high-rise social housing from the 1960s and 1970s, driven by a housing shortage, falls short of contemporary energy standards and creates challenges like electricity grid congestion. Short-term forecasting, enabled by PV forecasting, optimizes the performance of integrated PV and battery systems, contributing to sustainability goals and navigating urban energy complexities.

The ARV project specifically targets retrofitting eight residential buildings from the 1960s into PEBs. The integration of a smart grid with PVs, battery storage, and Vehicle-to-Grid assets supports the transition to positive energy structures. This serves as a model for sustainable energy solutions in Overvecht-Noord and Kanaleneiland-Zuid. The demonstration of this integrated approach in the pilot building, such as the PEB on the Henriettedreef, showcases the importance of the FFs in achieving ambitious sustainability targets. By studying flexibility in buildings equipped with PV and batteries and utilizing PV forecasting, the Dutch demo case maximizes self-consumption, peak shaving, and overall energy efficiency, paving the way for effective urban energy transformation.

Figure 18. PEB on the Henriette Dreef in Utrecht, a case study of Overvecht Noord District.

An essential aspect of achieving flexibility is accurate PV forecasting, which optimizes the performance of PV-battery systems. This is where the integration of sky imagers and the PV forecasting method becomes vital. Sky imagers are devices equipped with cameras that capture images of the sky at regular intervals (1s-1min, 1s). These images provide valuable information about cloud cover, cloud movement, and the position of the sun. By analysing the captured images, it becomes possible to estimate solar irradiance levels and predict PV output with greater accuracy. Sky imagers offer real-time data that can be utilized in short-term PV forecasting models.

The methodology employed in this research utilizes a machine learning model named Support Vector Machines (SVM) to enhance solar irradiance nowcasting. The process involves the pre-processing of the images captured to eliminate unwanted elements and create a camera-specific mask. The SVM classifier is trained using labelled training images to distinguish between cloud and sky pixels based on features such as colour ratios. The cloud mask obtained from the SVM classifier is then further processed to identify and track individual cloud objects. Cross-correlation algorithms are utilized to analyse the spatiotemporal relationships among cloud objects, enabling the determination of cloud motion and

cloud base height. Finally, the remaining pixels are classified as either cloud or clear sky, allowing for the extraction of solar irradiance data from the sky imagers. Figure 19 presents an overview of the cloud detection process.

Once the real-time data is obtained, it serves as a crucial input for the PV production forecasting model. To train the forecasting model, Global Horizon Irradiation (GHI) data is typically combined with corresponding PV production data. This training dataset is used to establish a relationship between GHI and PV production.
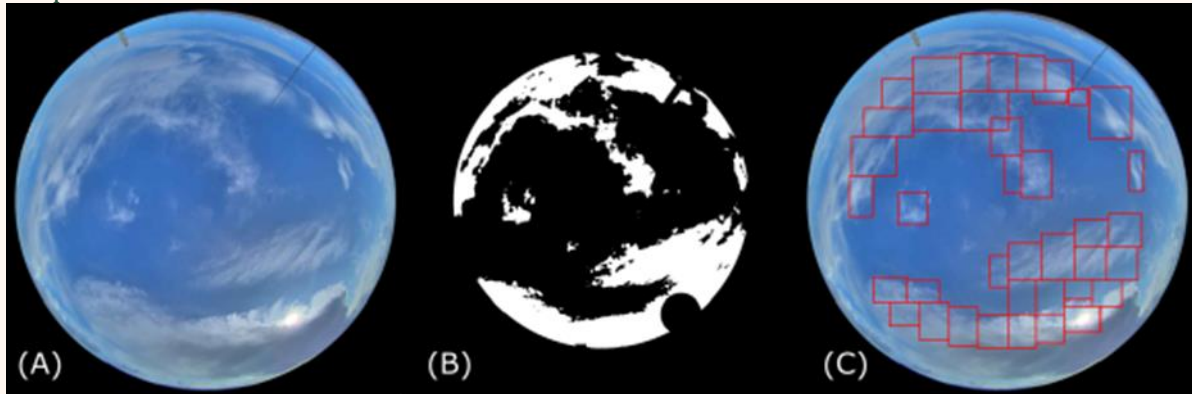

Figure 19. Figure (A) shows a photo that is analyzed by the SVM, figure (B) shows the cloud mask as identified by the SVM, figure (C) shows the corresponding cloud blocks that were determined.

During the training process, the model optimizes its internal parameters to minimize the difference between predicted PV production and actual measured PV production. This optimization helps improve the accuracy and reliability of the model's forecasts. Once the model is trained, it can be applied to new or future real-time GHI data to forecast PV production. The model takes the GHI values as input and generates predictions of the expected PV production levels. These predictions can be made for various time intervals, ranging from short-term forecasts (e.g., a few minutes ahead) to longer-term forecasts (e.g., a few hours or days ahead).

By continually updating the model with real-time GHI data, accurate forecasts of PV production can be generated for different time intervals. The success of this methodology depends on the quality of GHI measurements, the effectiveness of the forecasting model, and the continuous integration of the latest real-time GHI data to improve forecast accuracy and reliability.

4.6. CASE STUDY: BUILDING WITH THE PV SYSTEM AND BATTERY, OVERVECHT-NOORD DISTRICT, DUTCH

Towards sustainable energy solutions, integrating renewable energy, especially through PV systems, is gaining attraction in power grids. However, the variability of solar power presents challenges to electricity grid stability. To tackle this, energy storage technologies like batteries have become vital. This chapter explores insights, calculations, and the crucial role of flexibility in PV and battery systems, aiming to improve overall performance and adaptability in renewable energy integration for buildings. This aligns with the vision of creating climate-positive circular communities and promoting energy sustainability in residential areas.

Flexibility in PV systems means adjusting solar power generation to match dynamic grid demands, requiring advanced control strategies, predictive algorithms, and real-time monitoring. Similarly, flexibility in energy storage (batteries) involves efficient storage, discharge, and energy management. Scientific considerations include electrochemical processes and load management, with optimal flexibility requiring advances in battery control algorithms for enhanced efficiency, reliability, and lifespan.

The importance of flexibility for PV and batteries lies in overcoming the variability of renewable energy. The interdependence between PV systems and batteries is crucial for grid stability, energy reliability,

and sustainability. In the context of PV flexibility, short-term solar forecasting plays a vital role. Using sky imagers with a 180-degree fisheye lens, GHI and PV power output were forecasted through image processing. This forecasting, driven by machine learning algorithms considering real-time data and weather parameters, informs decisions on battery storage, ensuring they respond effectively to fluctuating energy demand and supply conditions, which, therefore, contributes to the seamless integration of solar energy into the power grid.

The case study building is 10 floors high and includes 58 apartments of different size, more specifically there are three different types, as shown in Figure 20. They have different size and room disposition: the one highlighted in green is the biggest with its six rooms, the orange one has five rooms, and the blue one only two rooms. They all have a window facing the building façade.

Figure 20. Apartment floor plans (technical drawings from the building design).

Furthermore, the building comprehends two facilities, which are the common areas that includes the elevators, the central heat-pumps, and all the common electrical appliances of the building. The roof has a roof (we call it pergola from now on), fully covered with Building Applied Photovoltaics (BAPV), with an asymmetric structure given by a compromise among the PV modules surface area, shading and the maximum allowed building height. The internal side of the pergola positioned towards South-East has a larger area than the side towards North-West. The two sides of the pergola which are the continuation of the façades are also covered with BAPV. The structure of the pergola can be seen in Figure 21 with two different figure orientations.
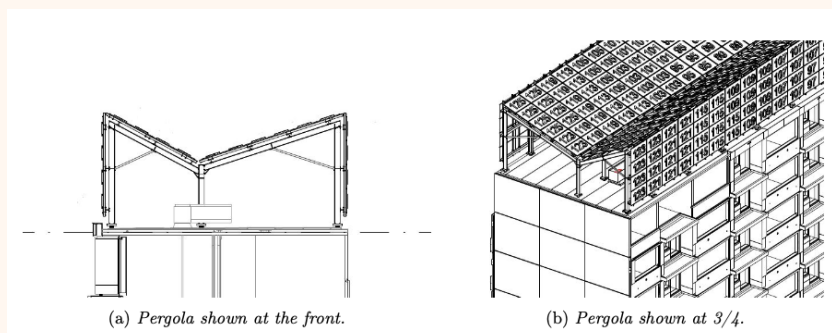

(a) *Pergola shown at the front.*   (b) *Pergola shown at 3/4.*

Figure 21. Structure of the pergola positioned on the roof (technical drawings from BOS).

The rest of the building, as the model in Figure 22 shows, is covered with BIPV. Specifically, the façade is composed by several balconies alternated to walls and the panels are located on both, also including the area below every window. Also, the lateral walls on the building are covered with BIPV.
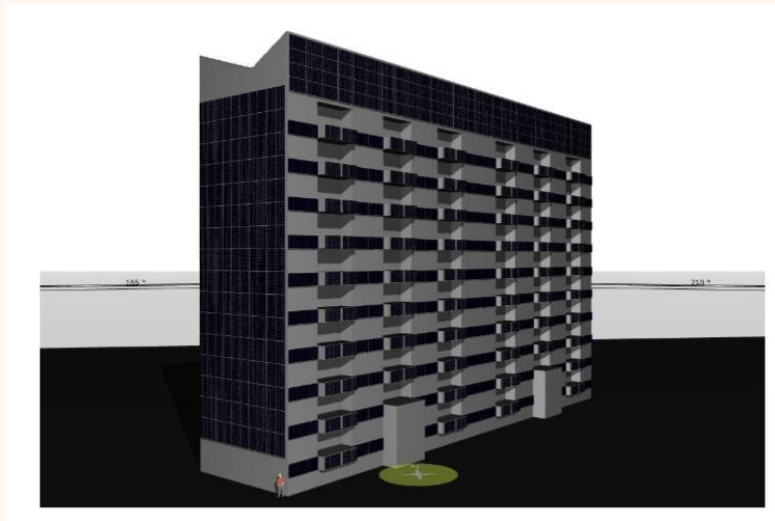
Figure 22. Modelled representation of the studied building (PVSites).

The building PV system is composed by 1 118 panels of different types. Figure 22 shows an overview of the panels positioning in the pergola. They differ in colour, as the majority of panels are black, with the exception of the ones on balconies which are transparent and below the windows which are coloured grey as the building wall. Then, they also differ in type, as the panels on the balcony and below the windows are BIPV, as already mentioned, with an individual capacity of 300 Wp, the modules on the inside of the pergola have an individual capacity of 355 Wp and the rest have an individual capacity of 340 Wp.

The number of panels from the pergola assigned to each apartment is depending on its characteristics (mainly, size and location), but each of them has its own inverter with 3 kW capacity, 58 in total, connected behind the energy meter (the device used to measure the amount of energy consumed) and cover the household electricity demand. The panels on balconies, façade, and side of the building are linked to separate inverters, which are seven and have a higher capacity, 7 kW or 17 kW. These larger inverters are responsible for the HVAC and Domestic Hot Water (DHW) demand of the building. The building is fully electric, meaning that it has been disconnected from natural gas supply and the district heating network. Heat pumps for both heating and DHW have been installed and electric stoves. A schematic of the electrical system of the building is detailed in Figure 23. The high-rise building's electricity system consists of connections to 58 residential apartments, and two sub-circuits connected to the facilities of the building. Table 4 provides further details on the specifics of the case study building and its installations.
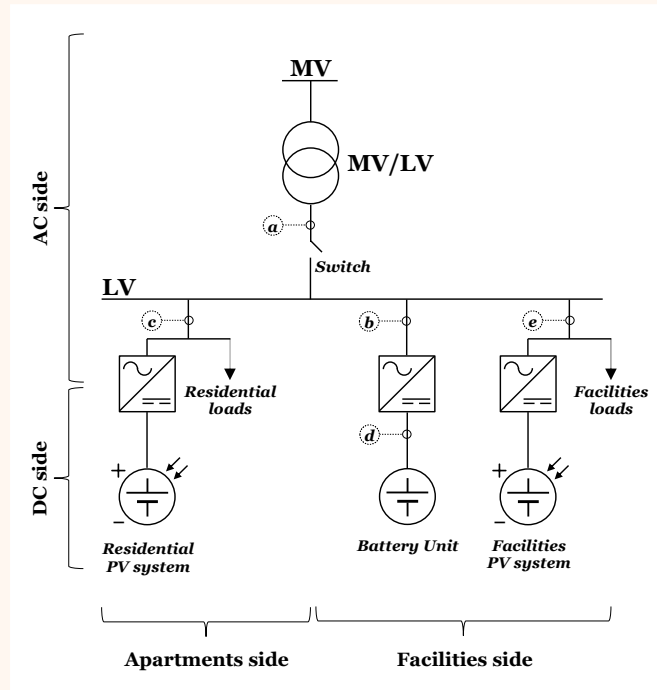
Figure 23. Schematic of the case study illustrating the connections to the grid with different systems within the building.

In this work, bidirectional electricity flows are assumed. At point a, power values are positive for the energy that flows from the MV/LV transformer to the building and negative if they flow from the building side to the MV/LV (therefore injected in the grid). At point e, we can ready the power values containing the facilities loads with the PV system and the Battery Energy Storage System (BESS). Therefore, with this line diagram we can determine all relevant power flows in the investigated system.

Table 4. Case Study Specifications

Main characteristics	Value	Unit
Number of apartments	58	-
Number of connections to facilities	2	-
Installed PV capacity (roof and façades)	360	kW$_p$
Nominal battery capacity	70	kWh
Battery discharge power	60	kW
Average building annual energy demand (2022)	200	MWh
Average annual PV production (2022)	255	MWh
Grid connection of the building's facilities	2x(3x80)	A
Grid connection of the building's facilities	110.4	kW
Grid connection of the apartment's	58x(1x35)	A
Grid connection of the apartment's	466.9	kW

Our comprehensive dataset incorporates inputs from smart meters that provide the annual energy usage by different components of the building including Apartments, Facilities as seen in Figure 24, providing valuable insights into energy use and PV production.
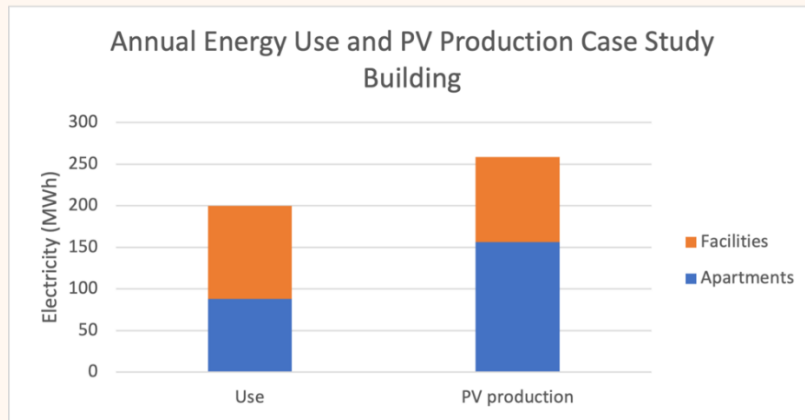
Figure 24. Annual energy use and PV production case study building (year 2022)

Two weeks of the year 2022 were analyzed to see the daily patterns more clearly and use the highest available time resolution, see Figure 25. Weeks in different seasons of the year were chosen. The number on the x-axis represents the hour of the year (out of 8760 hours per year).
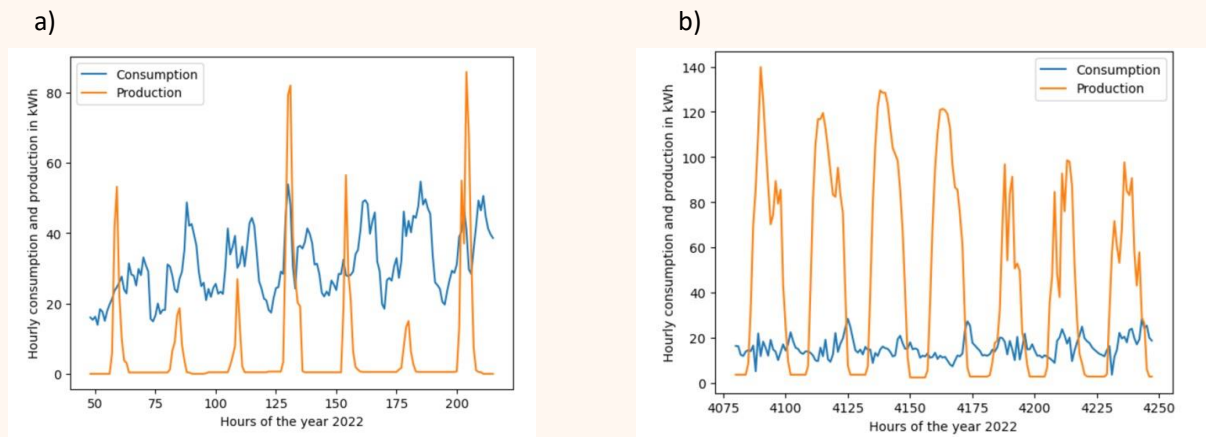
a)

b)

Figure 25. a) Hourly production and consumption in week 1 (January) of year 2022, b) Hourly production and consumption in week 25 (June 2022).

To provide a comprehensive understanding of the integration aspects of the FF of the PV and batteries, a high-level block diagram is presented in Figure 26. This diagram illustrates the key components involved in the process, including input data, the PV energy forecasts, battery optimization, and the simulation output of optimized battery profiles. The block diagram highlights the flow of information and processes within the integrated energy system. The input data consists of real-time data on solar irradiance, weather conditions, electricity prices, and energy demand. This data serves as the foundation for accurate PV energy forecasts and forms the basis for battery optimization.

The PV energy forecasts utilize advanced forecasting algorithms to predict the solar energy generation based on the input data. These forecasts enable proactive management of the PV system, allowing for efficient utilization of the generated energy and effective coordination with the battery system. The battery optimization process considers the objectives of maximizing peak shaving and self-consumption. Peak shaving aims to minimize peak demand by intelligently discharging the battery during high-demand periods. Self-consumption optimization focuses on maximizing the on-site utilization of PV-generated energy by appropriately charging and discharging the battery. The simulation output of optimized battery profiles represents the optimized operation of the battery system over a given time period. This output provides insights into the energy flows, battery charging and discharging patterns, and the overall performance of the integrated PV and battery system.

By integrating the input data, PV energy forecasts, and battery optimization model, the flexibility function of PV and batteries is effectively realized. This integration ensures adaptive responses to

changing energy demand and supply conditions, leading to enhanced efficiency, reduced peak demand, and increased self-consumption of PV-generated energy.
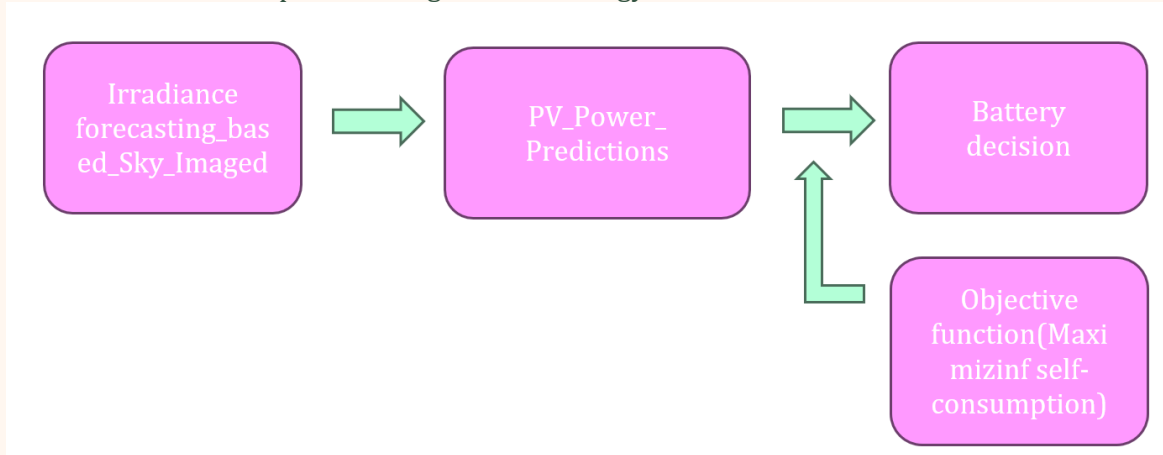

Figure 26. Illustration of the Flexibility function of PV and batteries

The high-level block diagram presented in Figure 26 provides a visual representation of the integration aspects involved in achieving the flexibility function of PV and batteries, showcasing the interconnectedness of the various components and processes within the system.

The objective function combines two terms, one for minimizing peak demand and the other for maximizing PV self-consumption. The peak demand term can be defined as the maximum power demand during a given time period (e.g., a day or a month). The optimization function equation takes into account both the energy use and the peak-demand. To minimize peak-demand, $f(x)$ is used as objective function to be minimized.

$$\min_{L(t)_{max} < x < L(t)_{min}} f(x)$$

$$f(x) = \left| C_{batt} - \left(max \int_{t_0}^{t} (L_i(t) - x)dt - min \int_{t_0}^{t} (L_i(t) - x)dt \right) \right|$$

where C_{batt} is the battery energy capacity, L_i is the load (i = a,b - power measured at point a or e, for the whole building aggregated or only facilities side respectively), x is the shave level. The PV self-consumption term SC_t can be defined as the percentage of PV energy that is consumed onsite, as opposed to being exported to the grid. $g(x)$ was used as objective function to be maximized:

$$max \, g(x)$$

$$g(x) = \sum_{t_0}^{t} SC_t \cdot dt$$

At the core of our investigation is an advanced short-term solar forecasting model, utilizing sky cameras and employing machine learning techniques to analyse images every 15 seconds. This model's primary objective is to forecast horizontal irradiance and predict PV power generation at the local level within the Demo buildings, considering an annual use and PV production of about 250 MWh, including facilities and apartments.

4.7. CASE STUDY: TURIN, ITALY

The first prototype of the novel shallow energy wall system was installed in 2018-2019 for experimental purposes to provide insight into the system energy performance and into the thermal impact that is exerted on the surrounding ground. It took place at the experimental facility of Energy Center Laboratory in Turin (Italy) and was characterized by three modular ground heat exchangers placed on an existing underground wall, see Figure 27. As regards the heating operations, it resulted that the system can continuously produce an exchange rate of 15-24 W/m^2 in winter and 26 W/m^2 in summer, in good agreement with expectation from similar systems known in literature. Sequential rather than parallel module linking was showed to weakly influence the thermal performance.

Figure 27. View of the GeothermSkin experimental test site (Baralis and Barla, 2021).

Based on thermal performance, the system is expected to provide a valuable contribution to the fulfilment of clean energy production from new and refurbished buildings. Furthermore, the system may be used in combination with other renewable energy sources (as the solar thermal panels) to make the housing completely self-sustaining. Consequently, the system may strongly contribute to the system energy flexibility due to its possibility to store heat from renewable sources.

The preliminary experimental results suggest that this very shallow geothermal system allow to obtain a satisfying amount of energy virtually not affecting the geothermal potential of deeper systems. The thermal status of the ground except for the very few meters from the system seems not to be noticeably altered. In this perspective the system may be adopted as a supplementary energy supplier beyond deeper installations as Borehole Heat Exchangers, open loop wells, energy piles and tunnels, virtually with a parallel exploitation. This kind of energy system may indeed play a role in the optimisation of the geothermal resources use, allowing to efficiently mine the heat at very shallow depths even in densely inhabited areas. At the moment, the demo is initiated and there is no yet results on the FF of the system.

The physical quantities related to the geothermal system functioning and the contextual climatic and soil variables monitored in the experimental site by the various sensors hide information on how the system works in real conditions. Such data were fed into a machine learning algorithm based on artificial neural networks, thus considering the resulting effects from unpredictable phenomena that cannot be modelled in a deterministic way. The volume of available data also conceals unknown and non-linear functional relationships that can be characterized through knowledge extraction processes based on data analysis. It is reasonable to assume that a relationship exists among the thermal heat rate transferred to the user, the climatic forces, and the state thermo-hygrometric measurements of the soil which would allow the heat rate to be estimated for heating produced by the geothermal heat pump for a generic combination of influencing variables. The artificial neural network is able to learn the connection and generalize it by acquiring forecasting skills with some margin of error for any combination of input variables, as long as they are within the training ranges. By providing the average

annual input variables of the Italian provinces it is possible to obtain an estimate of the thermal power that GeothermSkin would be able to achieve.

Predicted thermal power for an equipped area equal to that of the prototype (34.5 m²) has minimum values (959-1400 W) for Northern Italy where air and ground temperatures are colder and subject to wider seasonal variations despite benefiting from greater thermal capacity and thermal conductivity by virtue of the ground higher relative humidity. By dividing the total thermal power by the equipped surface, the average thermal power per unit surface is obtained. Dividing the required yearly thermal need per unit surface of building by the latter number, the area that has to be equipped with the GeothermSkin system per unit surface of building to fulfil the demand is obtained. Therefore, to preliminarily size the GeothermSkin system, first the building surface to be conditioned has to be estimated.

4.8. CASE STUDY: KARVINA HEALTHCARE CENTRE, CZECHIA

The Czech demo case is poised to serve as an exemplar and dynamic experimentation hub for pioneering innovations, with a strong potential for widespread adoption within Karvina and across the Czech Republic. At the core of the ARV project lies the objective to attain the nearly Zero-Energy Building (nZEB) standard, accomplished through a multifaceted approach combining rigorous building envelope renovations with the strategic implementation of advanced ARV innovations. These innovations encompass various technologies, including Building-Applied Photovoltaics (BAPV), Building-Integrated Photovoltaics (BIPV) systems, small-scale heat pumps, stationary second-life batteries, and Photovoltaic-Thermal (PV-T) collectors, each contributing synergistically to propel the building's performance beyond the nZEB benchmark. Figure 28 shows some photos of the implemented energy systems and their main characteristics are summarized in Table 5.

Figure 28. Installed renewable energy system in the demo Karvina.

Table 5. Karvina case main characteristics.

System – Specification	Value	Unit
Roof PV system (BAPV) size	29.58	kW_p
Façade PV system (BIPV) size	5.04	kW_p
Photovoltaic thermal collectores (PV-T) size	5.7 / 15.7	kW_{elc} / kW_{th}
Second-life battery capacity	50	kWh
Battery charge/discharge power	30	kW
Building annual average electrical demand	200	MWh
Building annual average thermal demand	900	MWh

To enhance the sustainability and flexibility of the building, a sophisticated high-level Smart Energy Management Strategy (SEMS) has been meticulously developed. This control strategy is designed not only to reduce energy expenses and operational costs but also to guarantee optimal technical performance and actively contribute to reducing grid congestion through ancillary services. The SEMS leverages PV and building load forecasting and day-ahead market electricity prices for the upcoming 24 hours as its primary inputs to operate the BSS with the objective of minimizing overall electricity expenses. A critical facet of this strategy involves interaction between the high-level and local controllers. This communication, synchronized with the selected sampling time for monitored data, ensures a continuous feedback loop. It allows for fine-tuning optimization decisions in response to real-time conditions, thereby addressing and mitigating the potential impact of forecasting inaccuracies. The general overview of the developed control strategy is shown in Figure 29.
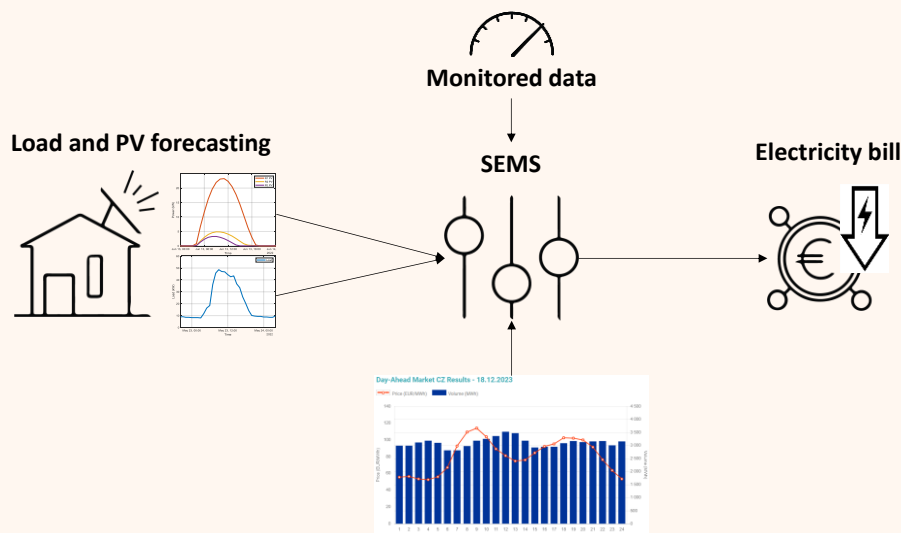

Figure 29. Smart energy management strategy working principles.

To assess the effectiveness of the proposed SEMS, the operation of the building has been simulated considering different scenarios. The simulation outcomes, incorporating technical parameters associated with peak-power importation/exportation to the grid, are depicted in Figure 30. In Part (a), the net energy duration curve reveals simulation outcomes tied to the building's operation when solely relying on PV installations without the energy storage system. Notably, the analysis indicates a maximum peak draw from the grid at 72.26 kW, with the highest surplus of PV energy sent to the grid reaching 21.95 kW. Moving to Part (b) of the same figure, the second scenario considers the results when incorporating the BSS operating under a conventional load-following control strategy (LFCS). While the peak power drawn from the grid remains consistent with the previous case, there is a marginal reduction in the excess peak power injected into the grid due to considering the BSS. The last segment

of the figure (Part (c)) displays outcomes derived from deploying the SEMS described above. Notably, the control strategy demonstrates enhanced ancillary services to the grid by limiting the power drawn from the grid to 60 kW. Additionally, the injected power into the grid is regulated while adhering to a specified maximum limit that the grid provider can set.
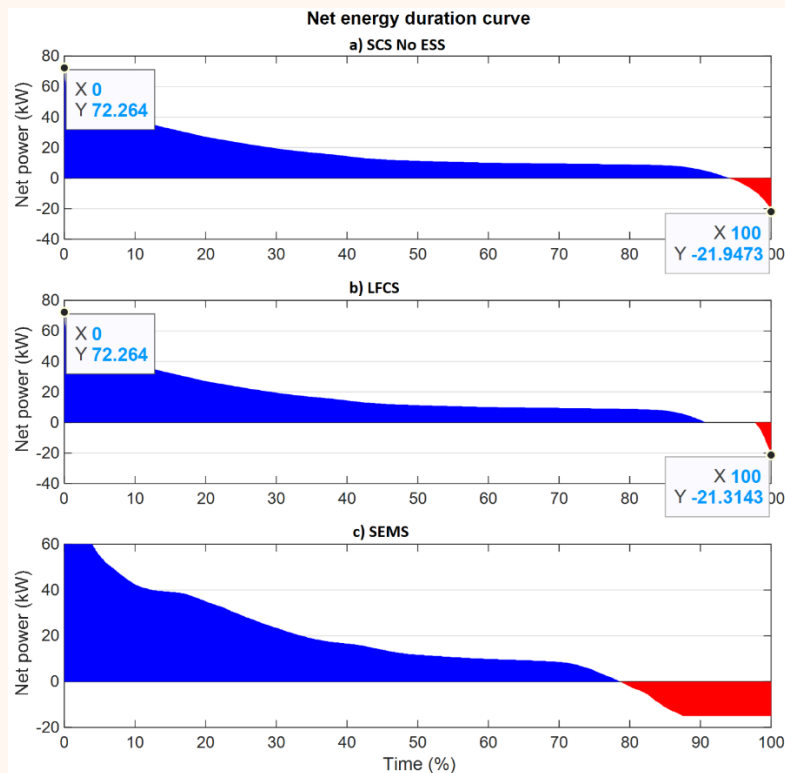

Figure 30. Net power importer/exported to the grid considering different control strategies of the energy systems.

Regarding the economic analysis of the building operating under the different scenarios, Figure 31 provides insights into evaluating the accumulated electricity bill over a year. The implemented Renewable Energy Systems (RESs) in the demo (mainly PVs and BSS) exhibit the potential to reduce the annual electricity cost by 20% from the baseline scenario, considering a conventional control strategy (such as LFCS). However, implementing the SEMS with the same setup further enhances the flexibility index, resulting in a at least 13% reduction – plus the rewards from the ancillary services provided to the grid – in the annual electricity bill compared to conventional control strategies.

Finally, some examples illustrating the detailed daily operation of the demo building based on the SEMS are given in Figure 32.
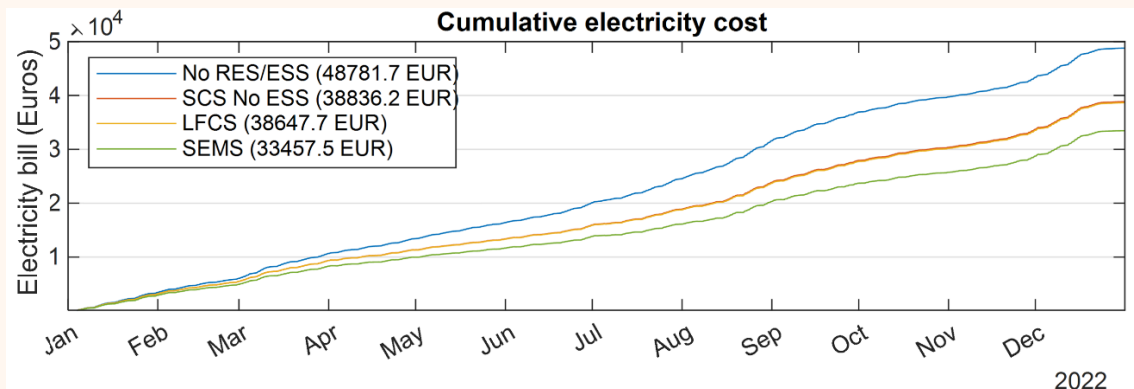

Figure 31. Cumulative annual electricity bill of the Karvina building operating under the different scenarios.
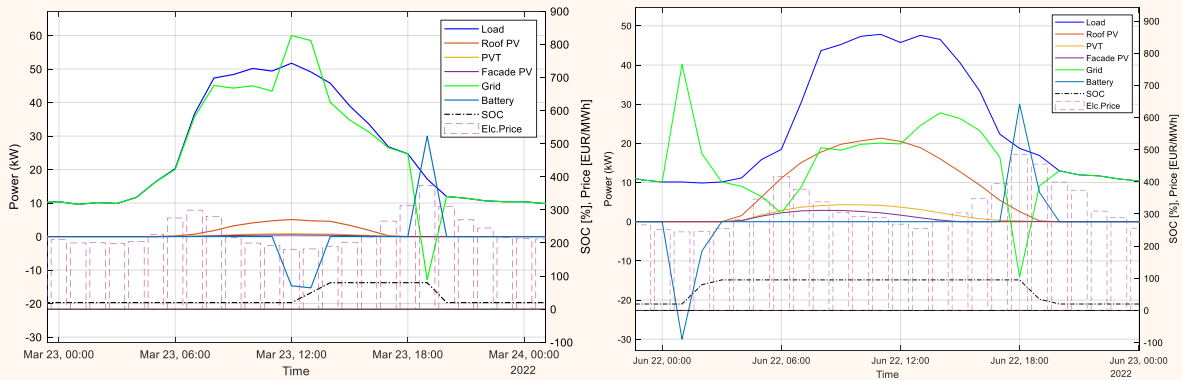
Figure 32. Examples of the building operating based on the SEMS.

Another big field to increase the flexibility index and reduce energy cost lies in the heating sector. The healthcare centre building is provided with heat by district heating. An additional experimental heating (and cooling) source was installed during the reconstruction on the roof of the building. This small reversible air-to-water heat pump provides heat and cold through radiation panels in the ceilings for six rooms in the 4th floor. The rest of the building is still supplied by the district heating.

Table 6. Heat pump and storage tank properties

System – Specification	Value	Unit
Heat pump el. power	3	kW
Heat pump seasonal COP	4	-
Heating water storage tank volume	400	l
Minimal tank water temperature	30	°C
Maximal tank water temperature	55	°C
(Estimated) annual average thermal demand of the 6 rooms	4,5	MWh

Since the heat pump has been installed quite recently, no real operational data are available yet. Hence, a following simulation case is considered – the thermal demand of the 6 rooms is estimated using the whole building thermal demand data from 2022. Furthermore, no cooling is considered since there is no historical data available, either. In cooperation with the heat pump, there is also a water storage tank with volume of 400 liters with heating water temperature constraints given in Table 6.

Using these assumptions an annual simulation has been carried out with the day-ahead price data from the Czech energy market operator (www.ote-cr.cz). The effective load shifting to reach the desired flexibility has been ensured by the MPC algorithm with a cost function to minimize the energy cost on the 8-hour prediction horizon while delivering the predicted heat demand. An overall scheme of the whole simulation is depicted in Figure 33.
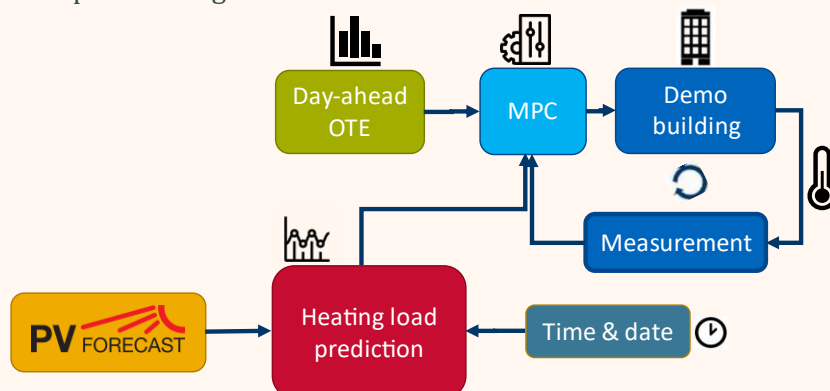

Figure 33. Czech demo - simulation scheme of the heat pump MPC to provide flexibility (part of the SEMS).

To assess the performance of this approach utilizing flexibility, the simulated MPC energy cost data were compared to the "baseline" original energy cost data (when considering the same dynamic price signal). In this small-scale heat pump control with implicitly provoked flexibility, the MPC reached approximately 16 % electricity cost reduction (only thanks to the control itself without considering any help from the PV or battery storage). The comparison of the cumulative heat pump electricity cost is shown in Figure 34.
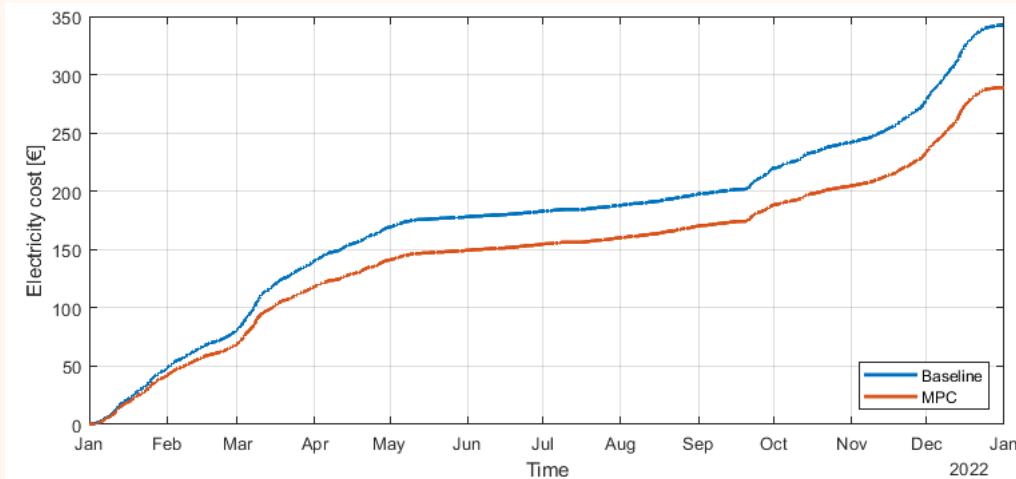

Figure 34. Czech demo - cumulative annual electricity bill of the small-scale heat pump operating under different control strategies.

Figure 35 provides a comprehensive illustration of the heat pump MPC operation and its performance throughout a single day. The algorithm efficiently prioritizes the heat production by the heat pump, aiming to coincide with the hours of lowest energy prices. This strategy maximizes the utilization of heat storage capacity while ensuring adherence to water temperature limits.
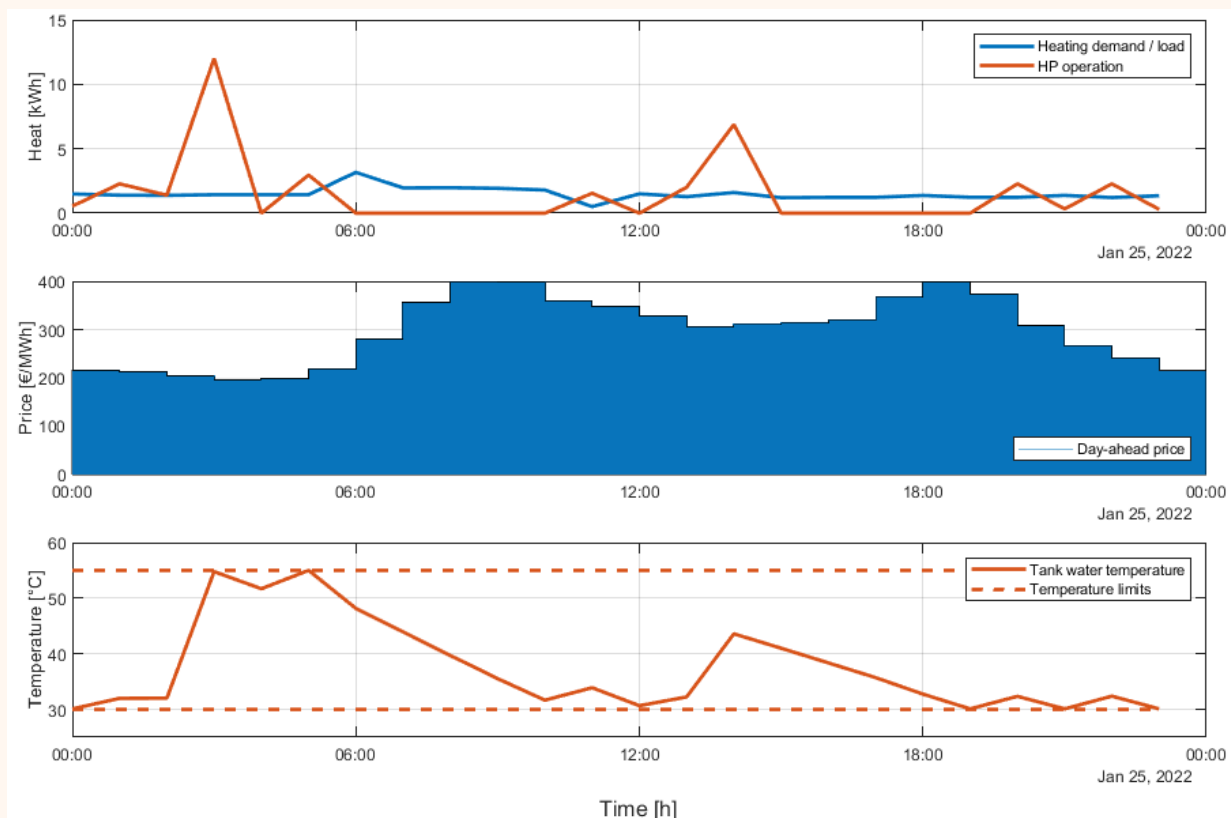

Figure 35. Czech demo - illustration of the heat pump MPC control during a winter day (simulation).

REFERENCES

1.   Junker, R.G., A.G. Azar, R.A. Lopes, K.B. Lindberg, G. Reynders, R. Relan, and H. Madsen, *Characterizing the energy flexibility of buildings and districts.* Applied Energy, 2018. **225**: p. 175-182; Available from: https://www.sciencedirect.com/science/article/pii/S030626191830730X.

2.   Junker, R.G., C.S. Kallesøe, J.P. Real, B. Howard, R.A. Lopes, and H. Madsen, *Stochastic nonlinear modelling and application of price-based energy flexibility.* Applied Energy, 2020. **275**: p. 115096; Available from: https://www.sciencedirect.com/science/article/pii/S0306261920306085.

3.   Tohidi, S.S., D. Cali, M. Tamm, J. Ortiz, and J. Salom. *From white-box to grey-box modelling of the heat dynamics of buildings.* in *BuildSim Nordic.* 2022. Copenhagen: accepted for publication.

4.   Tohidi, S.S., B. Eslami Mossallam, and D. Cali, *D4.1 Grey box models of the demonstration cases.* 2022, submitted report of the EU-project syn.ikia.

5.   Tohidi, S.S., H. Madsen, G. Tsaousoglou, and T.K.S. Ritschel *Adaptive flexibility function in smart energy systems: A linearized price-demand mapping approach.* Arxiv, 2023.

6.   Tohidi, S. and Y. Yildiz, *Handling actuator magnitude and rate saturation in uncertain over-actuated systems: A modified projection algorithm approach.* 2020.

7.   Tohidi, S.S., Y. Yildiz, and I. Kolmanovsky, *Adaptive control allocation for constrained systems.* Automatica, 2020. **121**: p. 109161; Available from: https://www.sciencedirect.com/science/article/pii/S0005109820303599.

8.   *Bygnings- og Boligregistret:* https://bbr.dk/forside.

9.   *DS-publikationstyper Dansk Standard udgiver forskellige publikationstyper. Typen på denne publikation fremgår af forsiden.* 2007

10.   *TABULA WebTool:* https://webtool.building-typology.eu/#bm.

11.   Tohidi, S.S., D. Cali, H. Madsen, N. Gaitani, H. Harter, T.H. Trulsrud, J. Salom, F.M. Lozano, M. Tamm, L. Hoes, R.v.d. Linden, W. Borsboom, and M. Ábel, *D4.2 Characterization of the thermodynamic properties of the demonstration cases.* 2022, submitted report of the EU-project syn.ikia.

12.   Eric, J., *CASE STUDY on Building level load shift potential* 01.12.2023

ACKNOWLEDGEMENTS AND DISCLAIMER

APPENDIX A – GLOSSARY OF TERMS

Flexibility function - FF
Positive Energy Buildings – PEB
Photovoltaic – PV
District Heating - DH
Global Horizon Irradiation – GHI
Building Applied Photovoltaics – BAPV
Domestic Hot Water – DHW
Battery Energy Storage System - BESS

PARTNER LOGOS

CLIMATE POSITIVE CIRCULAR COMMUNITIES

ARV